# กระบวนการไฮโดรทรีทติงแบบต่อเนื่องของผลิตภัณฑ์จากการกลั่นที่เป็นกรดไขมันปาล์มบนตัวเร่งปฏิกิริยาโลหะคู่ผสม NiCu/HZSM-5 เพื่อผลิตเชื้อเพลิงชีวภาพสำหรับอากาศยาน

นายพิสิษฐ์ วิริกุลเจริญ



วิทยานิพนธ์นี้เป็นส่วนหนึ่งของการศึกษาตามหลักสูตรปริญญาวิศวกรรมศาสตรมหาบัณฑิต
สาขาวิชาวิศวกรรมเคมี ภาควิชาวิศวกรรมเคมี
คณะวิศวกรรมศาสตร์ จุฬาลงกรณ์มหาวิทยาลัย
ปีการศึกษา 2560

# CONTINUOUS HYDROTREATING PROCESS OF PALM FATTY ACID DISTILLATE (PFAD) OVER BIMETALLIC NiCu/HZSM-5 CATALYST FOR BIO JET FUEL PRODUCTION

Mr. Phisit Wirikulcharoen



A Thesis Submitted in Partial Fulfillment of the Requirements
for the Degree of Master of Engineering Program in Chemical Engineering
Department of Chemical Engineering
Faculty of Engineering
Chulalongkorn University
Academic Year 2017

| | |
|---|---|
| Thesis Title | CONTINUOUS HYDROTREATING PROCESS OF PALM FATTY ACID DISTILLATE (PFAD) OVER BIMETALLIC NiCu/HZSM-5 CATALYST FOR BIO JET FUEL PRODUCTION |
| By | Mr. Phisit Wirikulcharoen |
| Field of Study | Chemical Engineering |
| Thesis Advisor | Professor Suttichai Assabumrungrat, Ph.D. |
| Thesis Co-Advisor | Assistant Professor Worapon Kiatkittipong, Ph.D. |

Accepted by the Faculty of Engineering, Chulalongkorn University in Partial Fulfillment of the Requirements for the Master's Degree

.....Dean of the Faculty of Engineering

(Associate Professor Supot Teachavorasinskun, D.Eng.)

THESIS COMMITTEE

.....Chairman

(Professor Bunjerd Jongsomjit, Ph.D.)

.....Thesis Advisor

(Professor Suttichai Assabumrungrat, Ph.D.)



.....Thesis Co-Advisor

(Assistant Professor Worapon Kiatkittipong, Ph.D.)

.....Examiner

(Assistant Professor Suphot Phatanasri, Ph.D.)

.....External Examiner

(Assistant Professor Kanokwan Ngaosuwan, D.Eng.)

พิสิษฐ์ วิริกุลเจริญ : กระบวนการไฮโดรทรีทติงแบบต่อเนื่องของผลิตภัณฑ์จากการกลั่นที่เป็นกรดไขมันปาล์มบนตัวเร่งปฏิกิริยาโลหะคู่ผสม NiCu/HZSM-5 เพื่อผลิตเชื้อเพลิงชีวภาพสำหรับอากาศยาน (CONTINUOUS HYDROTREATING PROCESS OF PALM FATTY ACID DISTILLATE (PFAD) OVER BIMETALLIC NiCu/HZSM-5 CATALYST FOR BIO JET FUEL PRODUCTION) อ.ที่ปรึกษาวิทยานิพนธ์หลัก: ศ. ดร.สุทธิชัย อัสสะบำรุงรัตน์, อ.ที่ปรึกษาวิทยานิพนธ์ร่วม: ผศ. ดร.วรพล เกียรติกิตติพงษ์, 59 หน้า.

งานวิจัยนี้ศึกษาตัวเร่งปฏิกิริยาโลหะผสมนิกเกิลและทองแดงบนตัวรองรับ HZSM-5 สำหรับผลิตเชื้อเพลิงชีวภาพสำหรับอากาศยานด้วยกระบวนการไฮโดรทรีทติง ตัวเร่งปฏิกิริยาที่มีอัตราส่วนนิกเกิลและทองแดงต่างกันถูกวิเคราะห์ด้วยเทคนิค ดังนี้ เอกซ์เรย์ดิฟแฟรกชัน โปรแกรมอุณหภูมิเพื่อทดสอบการคายซับของแก๊สแอมโมเนีย โปรแกรมอุณหภูมิเพื่อทดสอบการรีดักชันด้วยแก๊สไฮโดรเจน จุลทรรศน์อิเล็กตรอนแบบสแกนนิงและจุลวิเคราะห์ และการดูดซับทางกายภาพด้วยแก๊สไนโตรเจน กรดไขมันปาล์มเป็นส่วนที่ไม่สามารถรับประทานได้และเป็นของเหลือจากกระบวนการกลั่นน้ำมันปาล์ม ถูกนำมาใช้เป็นสารตั้งต้นในการศึกษานี้ สำหรับการคัดเลือกตัวเร่งปฏิกิริยา ได้ทำปฏิกิริยาในเครื่องปฏิกรณ์แบบกะภายใต้ อุณหภูมิ 375 องศาเซลเซียส ความดันแก๊สไฮโดรเจนเริ่มต้น 50 บาร์ เป็นเวลา 3 ชั่วโมง ผลการทดลองแสดงให้เห็นถึงการเติมทองแดงสามารถช่วยการเกิดปฏิกิริยาการดึงออกซิเจนออกและช่วยยับยั้งการก่อตัวของคาร์บอน และพบว่าการเติมนิกเกิลร้อยละ 12.5 โดยน้ำหนัก และ ทองแดงร้อยละ 2.5 โดยน้ำหนัก บนตัวรองรับตัวเร่งปฏิกิริยา HZSM-5 เป็นอัตราส่วนของตัวเร่งปฏิกิริยาที่มีความเหมาะสมเพื่อได้รับค่าการเปลี่ยนของกรดไขมันปาล์มสูงถึง ร้อยละ 94.8 กับ มีปริมาณคาร์บอนสะสมอยู่บนตัวเร่งปฏิกิริยาต่ำที่สุดประมาณร้อยละ 5 โดยน้ำหนัก โดยให้ค่าการเลือกเกิดของผลิตภัณฑ์เป็น แก๊สโซลีน ร้อยละ 14.9 เชื้อเพลิงสำหรับอากาศยาน ร้อยละ 45.0 และ น้ำมันดีเซล ร้อยละ 40.1 สำหรับการดำเนินการแบบต่อเนื่องตัวเร่งปฏิกิริยา นิกเกิลร้อยละ 12.5 โดยน้ำหนัก และ ทองแดงร้อยละ 2.5 โดยน้ำหนัก ถูกเติมลงบนตัวรองรับตัวเร่งปฏิกิริยา HZSM-5 ชนิดเม็ดที่จำหน่ายในเชิงพาณิชย์ ที่สภาวะการดำเนินงานอุณหภูมิ 400 เซลเซียส ความดันแก๊สไฮโดรเจน 40 บาร์ ปริมาณแก๊สไฮโดรเจนต่อปริมาณน้ำมัน 100:1 พบว่าค่าอัตราการไหลของสารตั้งต้นต่อปริมาตรของตัวเร่งปฏิกิริยา (LHSV) ที่เหมาะสมเท่ากับ 2 ต่อชั่วโมง ซึ่งมีค่าการเปลี่ยนสูง (ร้อยละ 90.1) และมีการดำเนินงานที่เสถียร โดยค่าการเปลี่ยนลดลงอย่างช้าๆ จนถึงเวลาที่ดำเนินการไป 80 ชั่วโมงจากเวลาเริ่มต้น (ค่าการเปลี่ยนเท่ากับ ร้อยละ 65.0) และ ลดลงอย่างรวดเร็วเหลือ ร้อยละ 36.5 ที่เวลา 103 ชั่วโมง



| | |
|---|---|
| ภาควิชา วิศวกรรมเคมี | ลายมือชื่อนิสิต ..... |
| สาขาวิชา วิศวกรรมเคมี | ลายมือชื่อ อ.ที่ปรึกษาหลัก ..... |
| ปีการศึกษา 2560 | ลายมือชื่อ อ.ที่ปรึกษาร่วม ..... |

# # 5870210021 : MAJOR CHEMICAL ENGINEERING

KEYWORDS: HYDROTREATING PROCESS / BIO JET FUEL / NICU/HZSM-5

PHISIT WIRIKULCHAROEN: CONTINUOUS HYDROTREATING PROCESS OF PALM FATTY ACID DISTILLATE (PFAD) OVER BIMETALLIC NiCu/HZSM-5 CATALYST FOR BIO JET FUEL PRODUCTION. ADVISOR: PROF. SUTTICHAI ASSABUMRUNGRAT, Ph.D., CO-ADVISOR: ASST. PROF. WORAPON KIATKITTIPONG, Ph.D., 59 pp.

This research investigated bimetallic NiCu/HZSM-5 catalyst for the production of bio jet fuel via hydrotreating process. The catalysts with different Ni and Cu ratio were characterized by XRD, $NH_3$-TPD, $H_2$-TPR, SEM-EDX and $N_2$-physisorption techniques. Palm fatty acid distillate (PFAD), nonedible by-product from palm oil refining process, was employed as a low-cost feedstock. For catalyst screening, the reaction was performed in an autoclave reactor under batch operation with operating temperature of 375°C, initial $H_2$ pressure of 50 bars and reaction time of 3 h. The results showed that doping Cu could enhance deoxygenation activity while carbon formation was found to be suppressed. 12.5 wt.% Ni and 2.5wt.%Cu doping on HZSM-5 catalyst was found as a suitable catalyst to obtain a high conversion of PFAD (94.8%) with the lowest carbon deposition on the catalyst (approx. 5 wt.%). The selectivity of green fuel is gasoline 14.9%, jet fuel 45.0% and diesel 40.1%. For continuous operation, 12.5 wt.% Ni and 2.5 wt.% Cu were loaded on commercial pellet-type HZSM-5 catalyst. At operating temperature of 400°C, $H_2$ pressure of 40 bar and $H_2$/oil molar ratio of 100, the most suitable LHSV of 2 $h^{-1}$ condition was found to achieve high conversion (90.1%) with a stable operation. The conversion gradually dropped over 80 h of the operating time (approx. 65.0% conversion) and then suddenly drops to 36.5% conversion at 103 h.



| | | |
|---|---|---|
| Department: | Chemical Engineering | Student's Signature ..... |
| Field of Study: | Chemical Engineering | Advisor's Signature ..... |
| Academic Year: | 2017 | Co-Advisor's Signature ..... |

# ACKNOWLEDGEMENTS

I really appreciate and would like to express my sincere thanks to my thesis advisor, Professor Suttichai Assabumrungrat and my co-advisor, Assistant Professor Worapon Kiatkittipong for their guidances and suggestions that are useful to this thesis.

I would also be grateful to Professor Bunjerd Jongsomjit as the chairman, Assistant Professor Suphot Phatanasri and Assistant Professor Kanokwan Ngaosuwan as the members of the thesis committee, for their useful comments and suggestions.

In addition, I am grateful to the scientists, my seniors, my friend, who are the members of Center of excellence on catalysis and catalytic reaction engineering, Chulalongkorn University and Research Center of Catalysis and Catalytic Reaction, Silpakorn University, for assistance, guideline and others. Especially, I would like to give my special thanks to Assistant Professor Worapon Kiatkittipong who always suggests everything which is beneficial throughout this thesis.

Finally, I most gratefully acknowledge my parents for consistent support and encourage me throughout the period of this research.

**CONTENTS**

Page

Page

Page

# LIST OF TABLES

Page

# LIST OF FIGURES

Page

Page

# Chapter 1
# Introduction

## 1.1 Introduction

Fossil has been employed as a main energy source until now. Not only fossil fuels shortages in the near future but also emission of CO2 lead to world problem such as global warming and climate change [1]. Green fuel production is one of the most effective ways to alleviate the problem especially in transportation sector. Bio fuel can be produced from various raw materials such as palm, corn, waste cooking oil, micro algae via various methods such as biodiesel, hydrothermal liquid fraction and hydrotreating.

Air freight transportation is the fastest and most reliable shipping method and accounting for around 10% of global transportation energy [2]. Around 1.5-1.7 billion barrel (47-53 billion gallons) of jet fuel per year was reported for the consumption of worldwide aviation industry [3]. Moreover, Fig 1 shows jet fuel consumption of Thailand per year, which increases continuously [4].

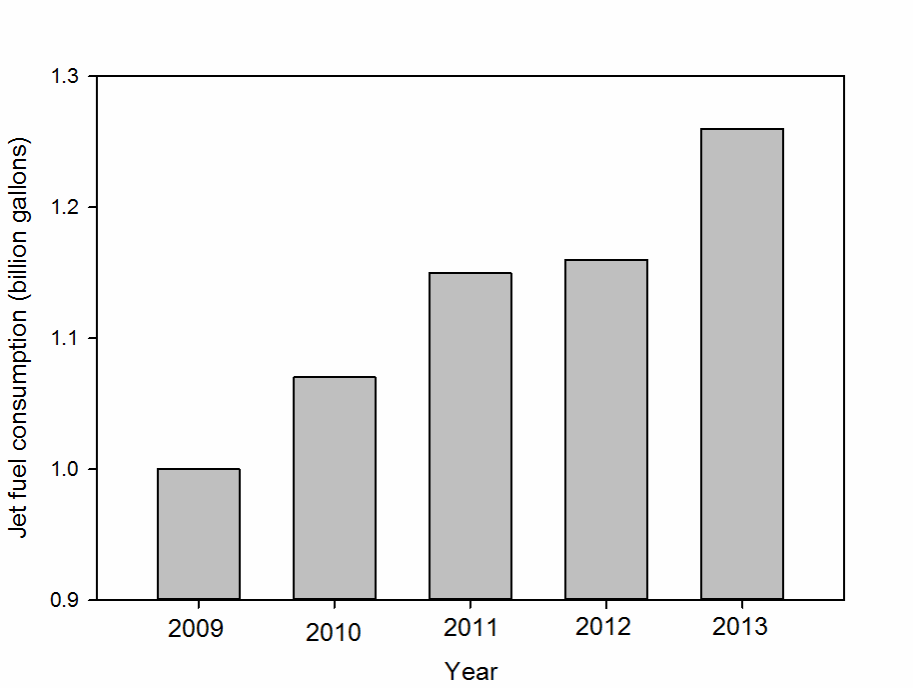


Fig. 1.1 Jet fuel consumption of Thailand in 2009-2013

Moreover, $CO_2$ emissions from aviation sector have been included in the EU emissions trading system (EU ETS) since 2012. This is critical as incremental of emissions costs. Expenses of ETS can be reduced by purchasing carbon credit of CERs (Certified Emission Reduction) from Clean Development Mechanism (CDM) [5, 6]

Hydrotreating is a suitable process for converting bio oil to biofuel because various products such as green diesel, bio jet fuel and gasoline can be obtained [1]. These products show the similar properties with fossil fuel, especially the heating value. Bio fuel, obtained from the hydrotreating process, can be utilized directly or blend together with conventional fossil fuel [7]. HZSM-5 has been proven as an effective zeolite catalyst for cracking [8]. This is because it provides lower coke formation and good thermal stability [9]. Ni catalyst demonstrated high activity and stability comparable to noble metals such as Pt, Pd and Ru [10]. In addition, Cu as co-catalyst, which was used with Ni-based catalyst, can significantly improve the activity, selectivity and stability for hydrodeoxygenation reaction [11].

The first generation biofuels are mainly obtained from edible crop plants. However, bio fuel manufacture from edible crops was affected to expensive raw material, this effect is called “Food Chain Material” [12]. Microalgae is non-edible and can grow in low space acreage, which has high lipid content, higher product/area ratio than other plants for produce bio oil. However, to achieve high, it requires high performance cultivation technology [13]. Waste oil is one of a most promising feedstock since low cost without changing in agricultural land use. Palm fatty acid distillate (PFAD), an inedible byproduct from palm oil refinery is of interest since oil palm is the most potential production among the existing Thailand's major oil crops.

## 1.2 Research Objectives

To produce bio jet fuel via hydrotreating process in single step reaction using Ni and Cu catalyst doping on HZSM-5

## 1.3 Scope of work

1.3.1 Perform catalysts screening in batch reactor, HZSM-5 with 15% loading metal catalyst on HZSM-5 with different Cu/Ni weight ratio (15Ni/HZSM-5, 10Ni5Cu/HZSM-5, 7.5Ni7.5Cu/HZSM-5) were tested at operating temperature of 375°C, $H_2$ pressure of 50 bar, reaction time of 3 h. Bio jet yield and carbon deposition on catalyst were evaluated.

1.3.2 Investigate the continuous hydrotreating process with selected NiCu/HZSM-5. LHSV was varied from 1-5 $h^{-1}$ at the temperature of 400°C, $H_2$ pressure of 40 bar, $H_2$/oil ratio of 100.

1.3.3 Bio jet fuel product was compared with ASTM D 1655.

**1.4 Research methodology**

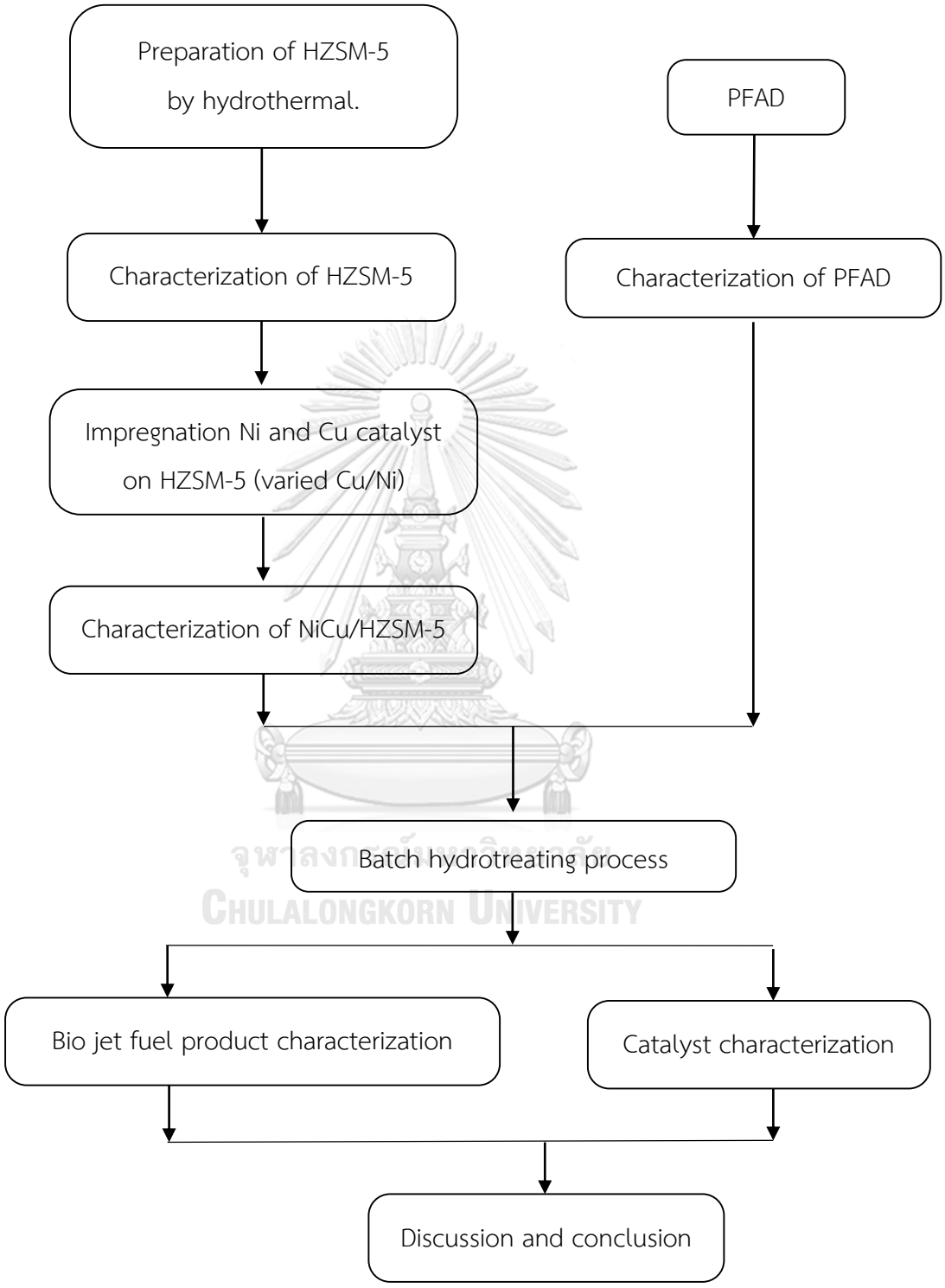




Fig. 1.2 Research methodology for screening catalyst

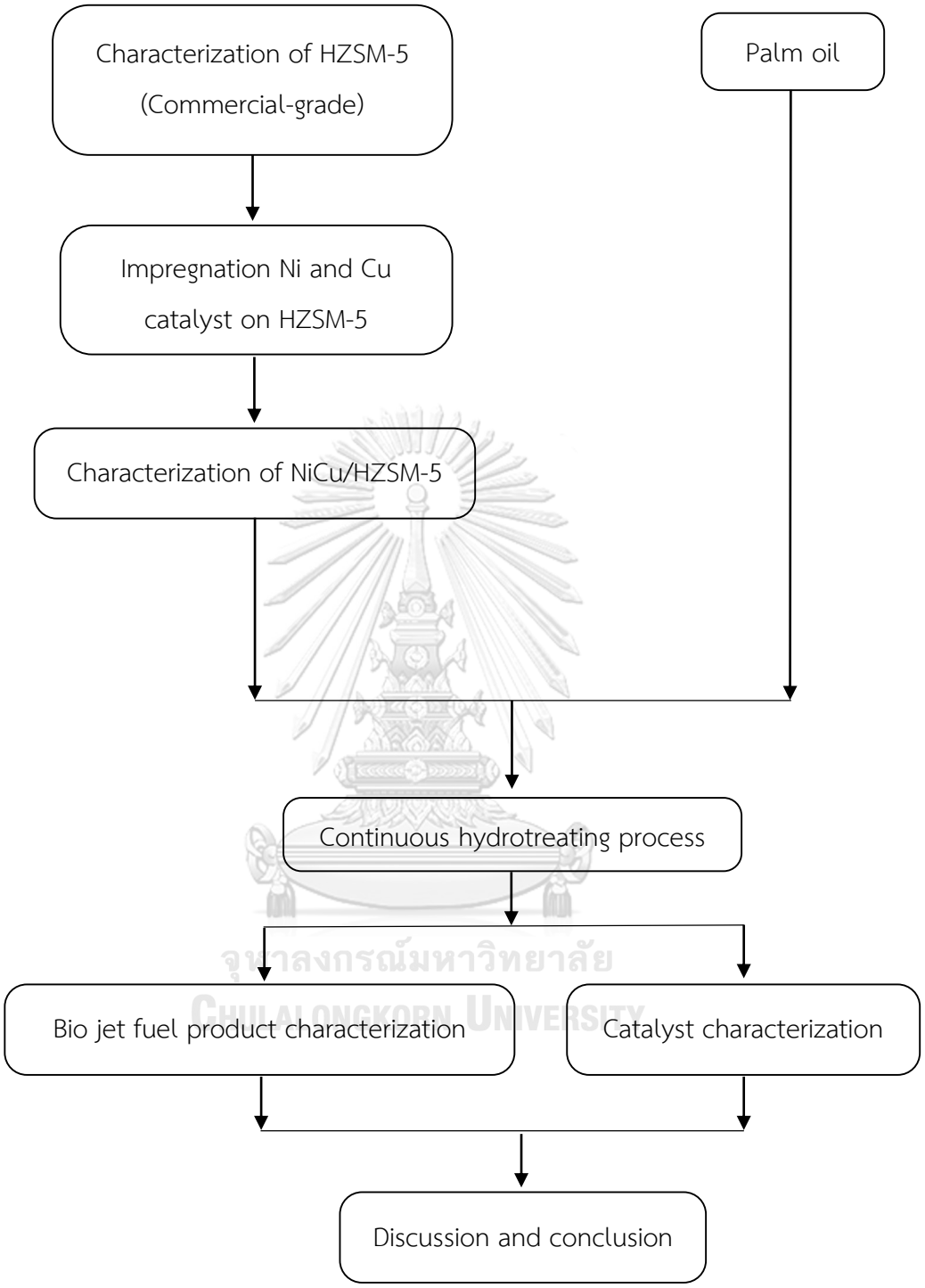




Fig. 1.3 Research methodology for continuous process

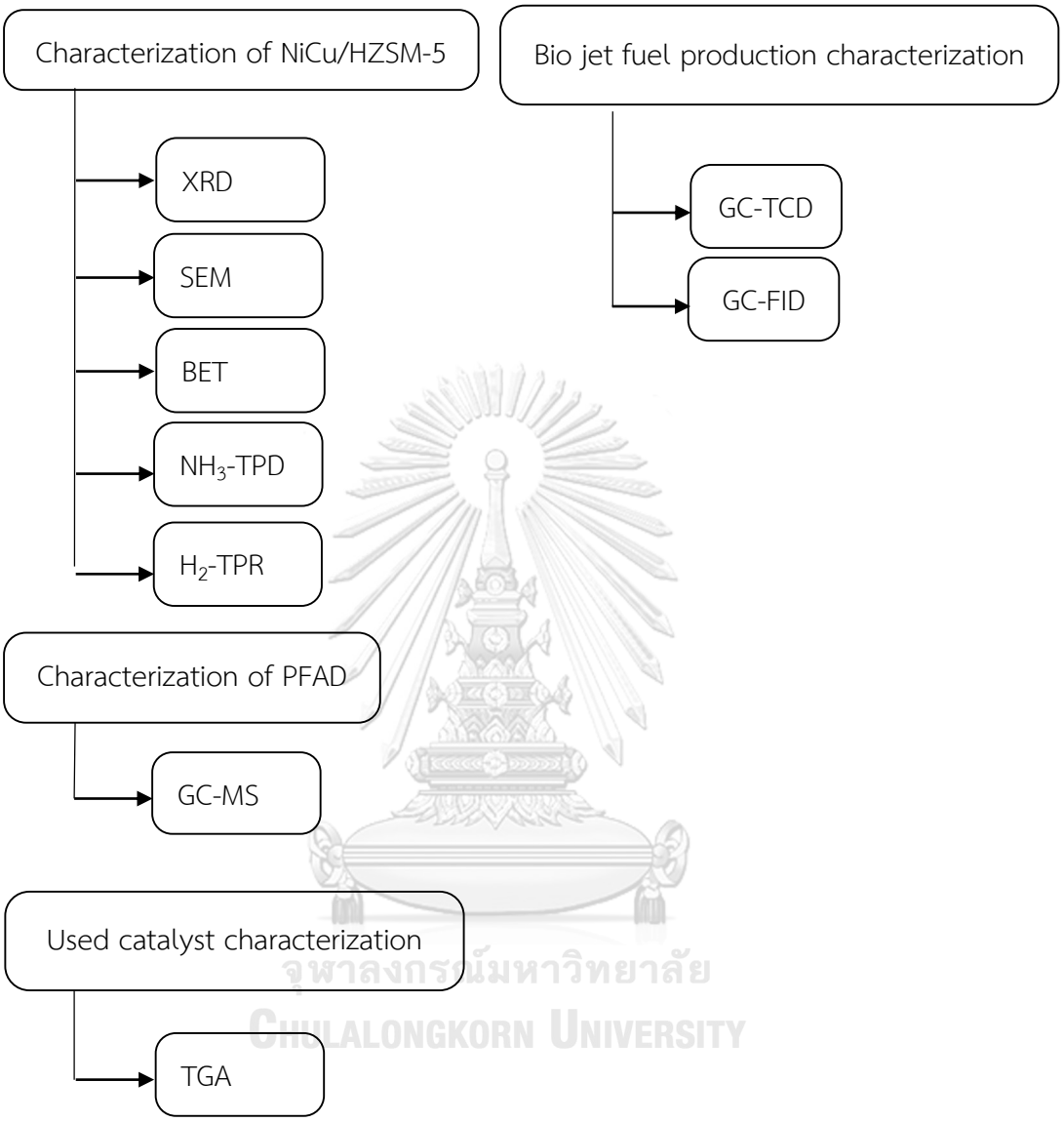




Fig. 1.4 Characterization methodology

# Chapter 2
# Theory

## 2.1 Bio jet fuel

Bio jet fuel is an alternative fuel from oils or animal fats through chemical process which its property closed to jet A or jet A-1 followed by American Society for Testing and Materials ASTM D 1655 and/or aviation turbine fuel containing synthesized hydrocarbons (hydroprocessed esters and fatty acids, HEFA) followed ASTM D 7566. This specification and detailed requirements of aviation turbine fuels are summarized in Table 2.1.

**Table 2.1** Detailed Requirements of Aviation Turbine Fuels

| Property | | D 1655 | D 7566 | ASTM Test Method |
|---|---|---|---|---|
| **COMPOSITION** | | | | |
| Acidity, total mg KOH/g | max | 0.1 | 0.10 | D 3242 |
| Aromatics, vol.% | max | 25 | 25 | D 1319 |
| | min | - | 8 | |
| Sulfur, mercaptan, weight % | max | 0.003 | 0.003 | D 3227 |
| Sulfur, total weight % | max | 0.3 | 0.3 | D 1266, D 1552, D 2622 |
| **VOLATILITY** | | | | |
| Distillation temperature, ℃: | | | | |
| 10 % recovered, temperature | max | 205 | 205 | D 86 |
| Final boiling point, temperature | max | 300 | 300 | D 86 |
| Distillation residue, % | max | 1.5 | 1.5 | D 86 |
| Distillation loss, % | max | 1.5 | 1.5 | D 86 |
| Flash point, ℃ | min | 38 | 38 | D 56 |
| Density at 15℃, kg/$m^3$ | | 775 to 840 | 775 to 840 | D 1289 |
| **FLUIDITY** | | | | |
| Freezing point, ℃ | max | -47 | -47 | D 2386 |
| Viscosity -20℃, $mm^2/s$ | max | 8 | 8 | D 445 |
| **COMBUSTION** | | | | |
| Net heat of combustion, MJ/kg | min | 42.8 | 42.8 | D 4529 |

| Property | | D 1655 | D 7566 | ASTM Test Method |
|---|---|---|---|---|
| One of following requirements shall be met: | | | | |
| (1) Luminometer number, or | min | 45 | - | D 1740 |
| (2) Smoke point, mm, or | min | 25 | 25 | D 1322 |
| (3) Smoke point, mm, and | min | 18 | 18 | D 1322 |
| Naphthalenes, vol, % | max | 3.0 | 3.0 | D 1840 |
| **CORROSION** | | | | |
| Copper strip, 2 h at 100°C | max | No.1 | No.1 | D 130 |
| **Contaminants** | | | | |
| Existent gum, mg/100 mL | max | 7 | 7 | D 381 |

## 2.2 Hydrotreating process

### 2.2.1 Reaction

Bio jet fuel can be produced by hydrotreating of triglycerides through two step processes: (1) adding hydrogen to remove oxygen from feedstock. There are three major reaction pathways including decarbonylation, decarboxylation and hydrodeoxygenation and (2) further refining the product to conform the jet fuel specifications such as heat of combustion, freezing point (these reactions are including isomerization and cracking), as showed in Fig. 2.1 [9, 14]. The $H_2$ consumption for hydrotreating of triglycerides can be ordered by the following: hydrodeoxygenation (HDO) > decarbonylation (DCO) > decarboxylation ($DCO_2$) [15].



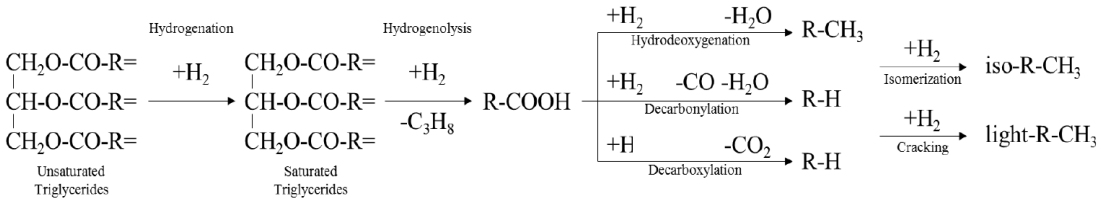


Fig. 2.1 Reaction pathway of hydrotreating process

Fig. 2.2 shows the potential energy diagram of hydrogen adsorption on Ni, Cu and NiCu surface. The hydrogen adsorption energies or activation barriers was reported in many literatures [16-18]. Each hydrogen molecule can easily adsorb on Ni surfaces,

while the hydrogen adsorption energies on Cu shows the value around 1.6 eV. The large difference of the binding energies of hydrogen bound to Ni and Cu makes the spillover of hydrogen from Ni to Cu energetically unpreferred. However, the hydrogen atoms on Ni sites could be supplemented from gas phase hydrogen after the hydrogen atoms spillover from hydrogen saturated Ni to Cu, the whole process is thermodynamically preferred, giving the hydrogen dissociative adsorption on Cu is exothermic process (0.2 eV). The spillover of hydrogen from Ni to Cu could be promoted by increasing the chemical potential of hydrogen on Ni, which could be achieved by increasing hydrogen adsorption pressure and temperature, or weakening the interaction between Ni and hydrogen [19].

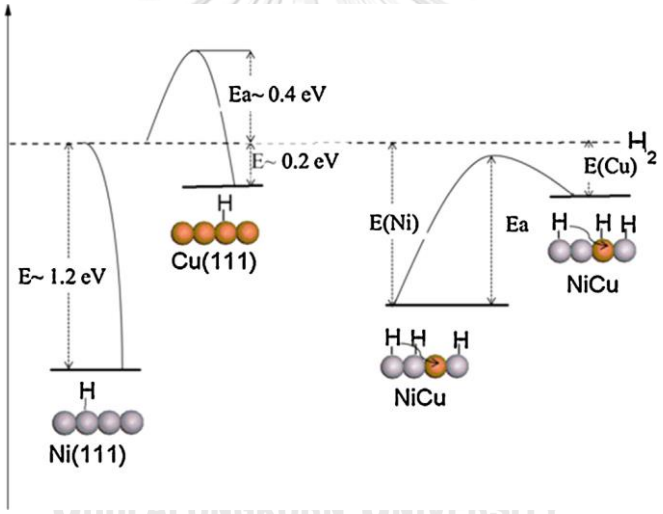


Fig. 2.2 Potential energy diagram of hydrogen on Ni, Cu and NiCu surface [19].

### 2.2.2 Catalyst

Zeolites catalyst, HZSM-5 has decency for catalytic cracking processes (change heavier component into smaller) because of it has highly crystalline, highly acidic, good activity and well-characterized zeolites. These active sites can promote decarboxylation and decarbonylation [20, 21]. Furthermore, low Si/Al ratio of HZSM-5 catalyst had high acid density which these could promoted isomerization and cracking [9].

Metal catalyst, often used in the deoxygenation of triglycerides are noble metals (Pt, Pd, Rh) and transition metals (Ni, Co) [22]. Moreover, the metal catalyst Pd, Pt and Ni were strongly promoted decarbonylation, decarboxylation reaction [23] and methanation reaction [14]. Noble metals showed high activity and stability but their high cost made the process for biofuels production ineffective on a large scale. On the other hand, the transition metals present a low cost and good activity as noble metal for upgrading bio oil [24, 25].

Moreover, addition of Cu to $Ni/ZrO_2$ catalyst showed a significant reduction in gasification activity, which increased the yield of HDO products (liquid hydrocarbon), preventing the formation of carbon and limiting the sintering on active phases of catalysts [26, 27]. The influence of modification of the Ni catalysts by Cu metals (geometry, electronic properties, and active sites) are in relation to their catalytic properties [26]. Nickel of Group VIII metal has free d-orbitals delocalized in the conductivity band and copper of Group 1B also has free d-electrons. Therefore, Ni interaction with the Group 1B metal caused the filling of d-zone [28].

**2.2.3 Operating conditions**

The HDO pathway is exothermic reaction which should be operated at low temperature. However, the DCO and $DCO_2$ pathway are endothermic reaction which not followed the trend of HDO pathways. Therefore, it should be investigated temperature of three major pathways to find optimal condition [14]. Moreover, high temperature was promoted cracking and isomerization due to there are endothermic reactions [29].

The adsorbed hydrogen on active sites surface of catalyst is the function of the hydrogen pressure, the increase of hydrogen pressure raised the solubility of hydrogen in reactant (vegetable oil) across the catalyst surface. The HDO reaction is the main pathway due to the larger amount of hydrogen at active site [14].

Moreover, the increase in contact time (low LHSV) lead to higher product yield and high iso/normal alkane ratio because of allowing longer contact time between reactant and catalyst [14].

### 2.3 Raw material (biomass)

Currently, there are several kinds of raw materials for bio fuel production such as palm, corn, soybean, algae and other. However, these raw materials were not satisfying because use edible vegetable oil to produce bio fuel was caused some concern in the food chain material affecting the increased in raw material prices. Palm fatty acid distillate (PFAD) was interested as one of a potential feedstock because PFAD was nonedible crops and it was a by-product from palm oil refinery. The fatty acid compositions of PFAD are similar to palm oil as summarized in Table 2.2 [14] [30].

**Table 2.2** Fatty acid compositions of palm oil and PFAD

| Fatty acid | Formula | Compositions (wt.%) | |
|---|---|---|---|
| | | Palm oil | PFAD |
| Lauric acid | $C_{12}H_{26}O_2$ | 0.4 | - |
| Myristic acid | $C_{14}H_{28}O_2$ | 0.8 | 1.1 |
| Palmitic acid | $C_{16}H_{32}O_2$ | 37.4 | 49.0 |
| Palmitoleic acid | $C_{16}H_{30}O_2$ | 0.2 | 0.2 |
| Stearic acid | $C_{18}H_{36}O_2$ | 3.6 | 4.1 |
| Oleic acid | $C_{18}H_{34}O_2$ | 45.8 | 35.8 |
| Linoleic acid | $C_{18}H_{32}O_2$ | 11.1 | 8.3 |
| Linolenic acid | $C_{18}H_{30}O_2$ | 0.3 | 0.3 |
| Arachidic acid | $C_{20}H_{40}O_2$ | 0.3 | 0.3 |
| Eicosenoic acid | $C_{20}H_{38}O_2$ | 0.1 | 0.2 |
| Tetracosenoic acid | $C_{24}H_{46}O_2$ | - | 0.6 |



### 2.4 Catalyst deactivation

A major problem of hydrotreating process is deactivation of catalyst via loss of active site. There are many causes including poisoning, coking or fouling, phase transformation.

Poisoning causes the loss in activity due to the strong chemisorption on the active site of impurities in the reactant. A poison could be blocking an active site or may alter the absorptivity of other species essentially by an electronic effect. Moreover, poisons can change the chemical nature of active site or result in the formation of new compounds, so that the catalyst performance is definitively altered [31]. A conceptual two-dimensional model of sulfur poisoning of ethylene hydrogenation on a metal surface is shown in Fig. 2.3 [32].

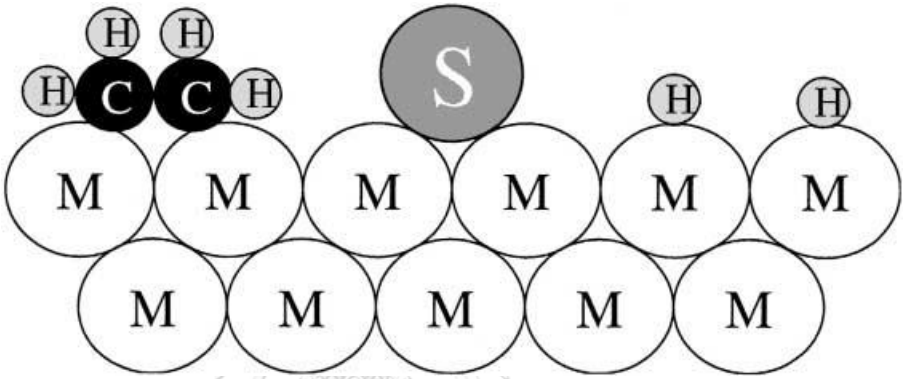


Fig. 2.3 Conceptual model of poisoning by sulfur atoms of a metal surface during ethylene hydrogenation [32].



Fouling is one of the causes for catalyst deactivation. Fouling is the physical deposition of species from fluid phase on the catalyst surface, which results in activity loss due to blockage of sites and pores. Mechanical deposition of carbon and coke in porous catalyst were forming processes also involve chemisorption of different kinds of carbons or condensed hydrocarbons. Typically, carbon is a product of CO disproportionation while coke is produced by decomposition or condensation of hydrocarbon on catalyst. Possible effects of fouling by carbon or coke on the functioning of a supported metal catalyst were showed in Fig. 2.4. Carbon might be (1) chemisorb strongly as a monolayer or physically adsorb in multilayers and in either case block access of reactants to metal surface site, (2) totally encapsulate a metal particle and thereby completely deactivate that particle and (3) plug micro and

mesoporous such that access of reactants is denied to many crystallites in side these pores. Finally, in extreme cases, strong carbon filaments may build-up in pores to the extent that they stress and fracture the support material, ultimately causing disintegration of catalyst pellets and plugging of reactor voids [32].

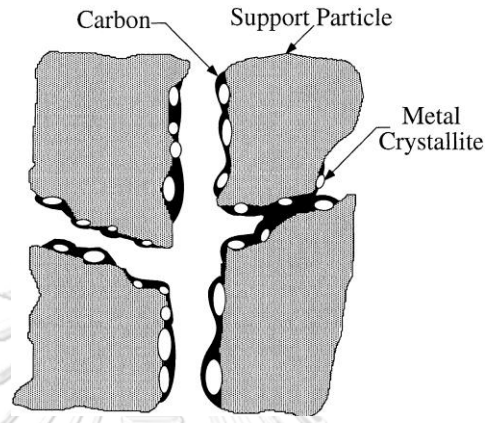


Fig. 2.4 Conceptual model of fouling, crystallite encapsulation and pore plugging of a supported metal catalyst due to carbon deposition [32].

Sintering is thermally induced deactivation of catalyst results from (1) loss of catalytic surface area due to crystallite growth of the catalytic phase, (2) loss of support area due to support collapse and of catalytic surface area due to pore collapse on crystallites of the active phase. The processes of crystallite and atomic migration as shows in Fig. 2.5 [32].



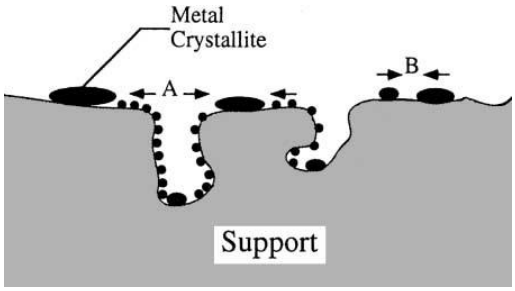


Fig. 2.5 Two conceptual models for crystallite growth due to sintering by (A) atomic migration or (B) crystallite migration [32].

Coke deactivation is a main cause in hydrotreating process by hydrocracking reaction which is the breakdown of a large molecule into smaller, especially at high temperature. These coke affected to the activity, selectivity and stability of the catalyst because coke formed on the catalyst which blocked access reactant to active sites [31, 33].

# Chapter 3
# Literature review

## 3.1 Bio fuel

Currently, the bio fuel from biomass consists of two major process which are biodiesel and deoxygenation process. Biodiesel is product from transesterification and esterification process of triglycerides with methanol. Biodiesel or fatty acid methyl esters (FAMEs) has C=C bond and C=O bonds remaining in the molecules. Therefore, biodiesel shows low thermal stability, low heating value, high viscosity and low oxidation stability because of its high oxygen content and unsaturated bond. On the other hand, green fuel or production from deoxygenation process has better properties than those of biodiesel such as high cetane number, zero oxygen containing, high thermal stability and high oxidation stability [23].

Biodiesel has the similar combustion properties with petroleum diesel, but biodiesel had more unsaturated bonds and showed higher oxygen content than petroleum diesel. Catalytic cracking could decrease oxygen content in molecular structure. Consequently, hydroprocessing is the key for development of technologies to produce renewable bio fuels [34].



## 3.2 Deoxygenation process

There are many literatures about deoxygenation process such as: changing feed stock in process for appropriate in each region, find optimum condition in process (Temperature, $H_2$ Pressure, LHSV, feed rate) and find suitable catalyst for deoxygenation reaction. Al-Muhtaseb *et al.* [35] used date pits for supported catalyst and bio oil in deoxygenation process. Owing to date pits are considered as one of the major agricultural wastes in Oman. Guo *et al*. [26] studied about using algae bio oil in catalytic hydrodeoxygenation. The algae bio oil was interested in this process because the length of hydrocarbon in the algae bio oil was in range of $C_7$-$C_{17}$ and the oil boiling point was approximately 100-300°C. Date pits oil and algae bio oil have high lipid

contents, thus, the two oils were suitable to be used in the process as Srifa *et al.* [14] used palm oil (feed stock) in catalytic hydrotreating. In Thailand, palms are the major industrial crops to produce palm oil in palm oil refinery, which this process has palm fatty acid distillate (PFAD) as by-product. That causes PFAD was interested as raw material for value added by catalytic hydroprocessing to produce green fuel.

In part of reaction condition and catalyst, Chen *et al.* [9] used 10Ni/HZSM-5 with reaction conditions at 280°C, $H_2$ pressure of 0.8 MPa, LHSV of 4 $h^{-1}$ and highly purified $H_2$/oil molar ratio of 15. The 10 wt.% Ni/HZSM-5 provided a high selectivity of 88.2% for $C_5$-$C_{18}$ liquid alkane, which liquid alkane has 8% of gasoline alkane, 32.5% of jet alkane and 47.7% of diesel alkane. The interesting point in this research was 10Ni/HZSM-5 reported high content of carbon deposition after operation of 80 h that resulting in the decrease in the conversion of FAMEs to 30.1%. Guo et al. [26] studied the catalytic hydrodeoxygenation of algae bio oil over NiCu/$ZrO_2$ catalyst with reaction condition at 350 °C, $H_2$ pressure of 2 MPa. This catalyst showed the highest activity of HDO efficiency of 82% for 15.71Ni6.29Cu/$ZrO_2$ catalyst, which had higher HDO efficiency than S-NiMo/$Al_2O_3$ catalyst and lower coke deposit on catalyst. Thus, the addition of Cu with Ni catalyst could promote the increasing of HDO efficiency and decreasing of coke deposit on catalyst. For noble metal, Sotelo-Boyás *et al.* [29] studied about noble metal catalyst compared with bimetal catalyst for renewable diesel production from the hydrotreating. The interesting result in this work was the bimetal catalyst (NiMo/$Al_2O_3$) showed lower yield of diesel than noble metal catalyst (Pt-HY) due to the less acidity of Pt-HY. The research of Srifa et al. [23] showed catalytic activity was in the order of Co > Pd > Pt > Ni for green diesel production in hydrodeoxygenation of palm oil.



Moreover, there are many researches in the topic of green fuel or deoxygenation as well. They investigated about reaction condition, catalyst, feed stock and process as shows in Table 3.1 (Batch process) and Table 3.2 (Continuous process).

**Table 3.1** Batch process

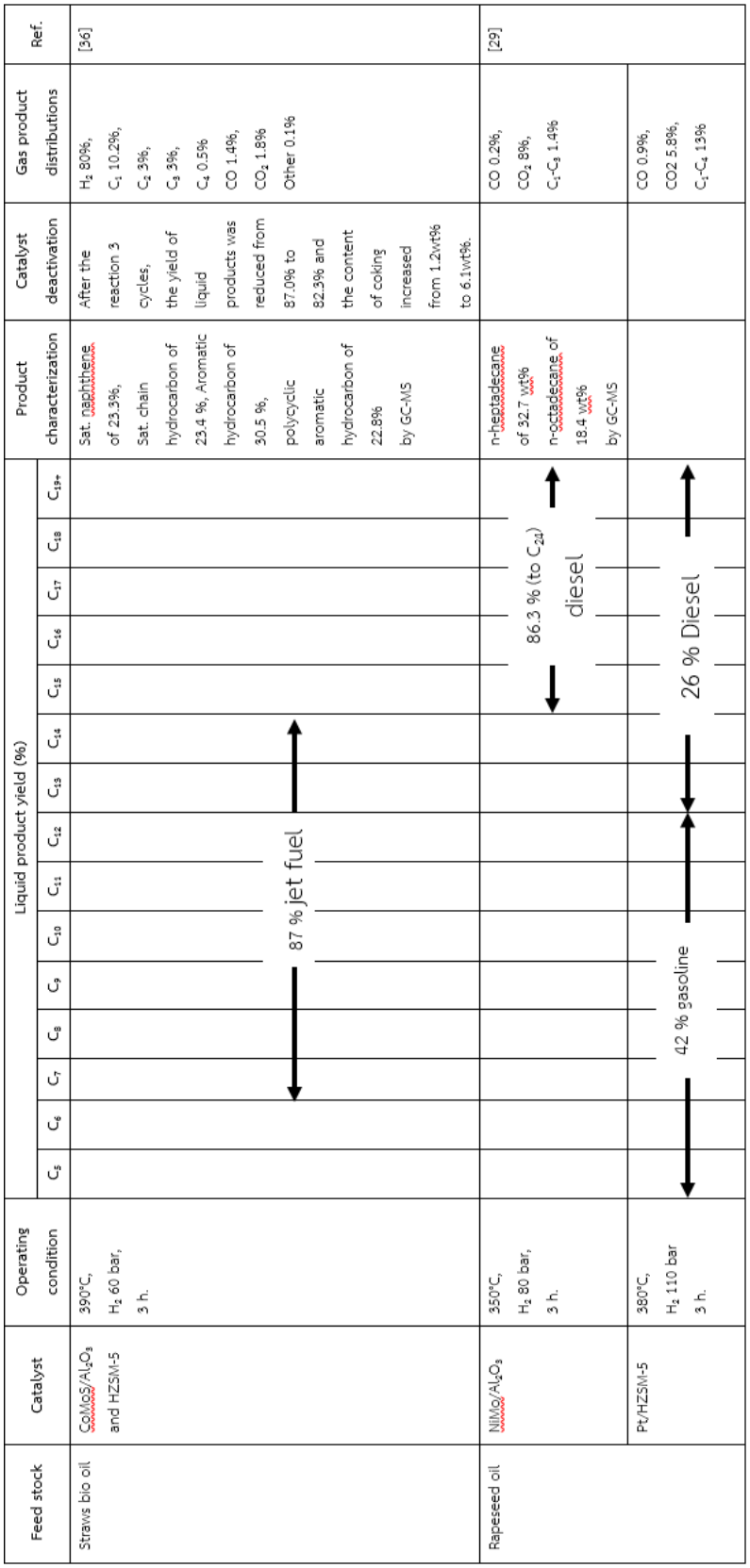

| Feed stock | Catalyst | Operating condition | Liquid product yield (%) | | | | | | | | | | | | | | Product characterization | Catalyst deactivation | Gas product distributions | Ref. |
|---|---|---|---|---|---|---|---|---|---|---|---|---|---|---|---|---|---|---|---|---|
| | | | $C_5$ | $C_6$ | $C_7$ | $C_8$ | $C_9$ | $C_{10}$ | $C_{11}$ | $C_{12}$ | $C_{13}$ | $C_{14}$ | $C_{15}$ | $C_{16}$ | $C_{17}$ | $C_{18}$ | $C_{19+}$ | | | | |
| Soybean oil | $Ni/SiO_2$-$Al_2O_3$ | 400°C, $H_2$ 92 bar, 1 h. | | | | | | | | | | | ← 39.3 % → | | | | | The much smaller n-alkane content may suggest that the formation of iso-alkane, cycloalkanes, or aromatic carbon species was enhanced by the NiMo catalyst | | $H_2$ 60%, $C_2$-$C_4$ 8% CO 2%, $CO_2$ 30% Of $NiMo/\gamma$-$Al_2O_3$ (higher performance) | [36] |
| | Pd/γ-$Al_2O_3$ | | | | | | | | | | | | ← 48.3 % → | | | | | | | | |
| | Pt/γ-$Al_2O_3$ | | | | | | | | | | | | ← 57.8 % → | | | | | | | | |
| | $Ru/Al_2O_3$ | | | | | | | | Diesel | | | | ← 86.4 % → | | | | | | | | |
| | CoMo/γ-$Al_2O_3$ | | | | | | | | | | | | ← 67.1 % → | | | | | | | | |
| | NiMo/γ-$Al_2O_3$ | | | | | | | | | | | | ← 91.0 % → | | | | | | | | |
| Palm kernel fat | Pd/C | 300°C $H_2$ 10 bar 5 h. | | | | | | ← | | | 92.0 % (to $C_{25}$) Diesel | | | | | → | | | | | [29] |

**Table 3.2** Continuous process

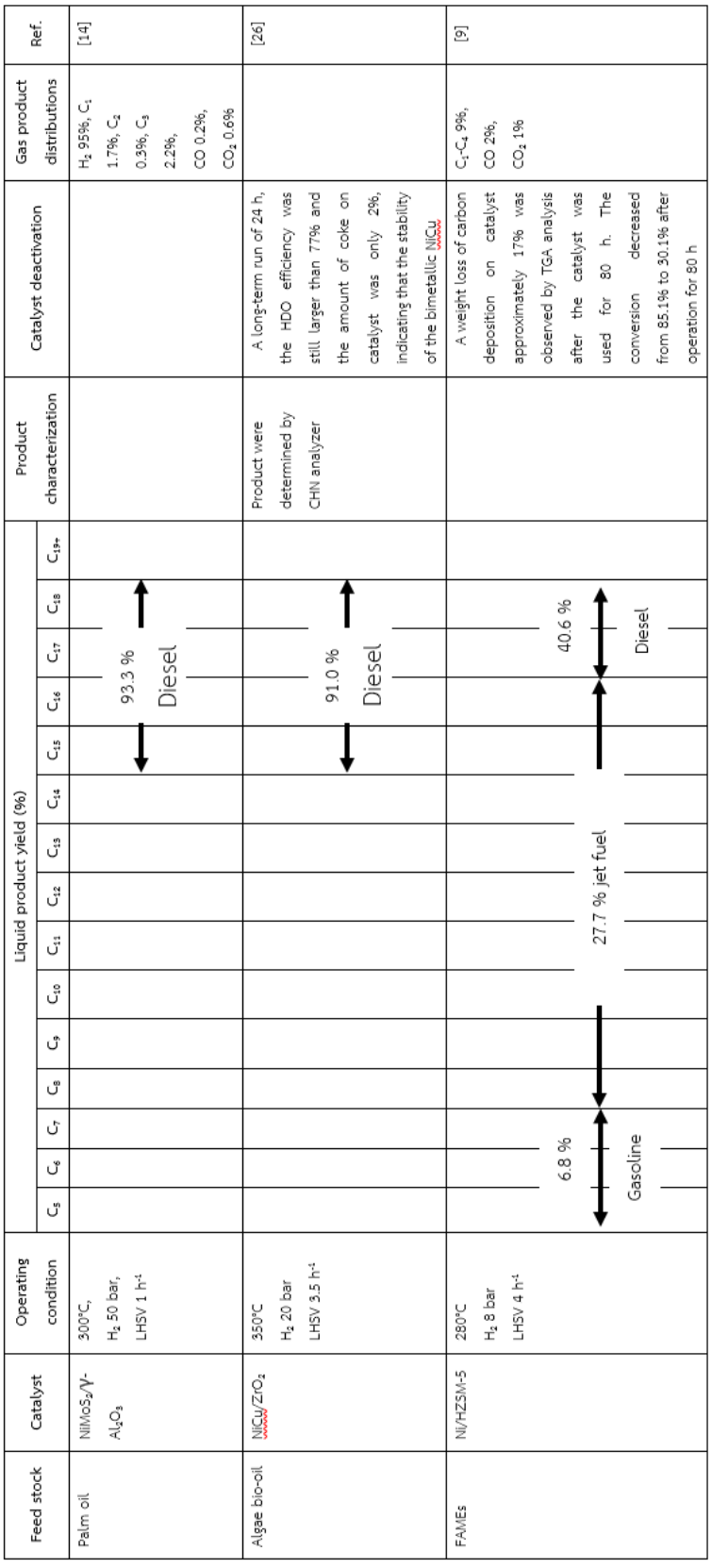

| Feed stock | Catalyst | Operating condition | Liquid product yield (%) | | | | | | | | | | | | | | Product characterization | Catalyst deactivation | Gas product distributions | Ref. |
|---|---|---|---|---|---|---|---|---|---|---|---|---|---|---|---|---|---|---|---|---|
| | | | $C_5$ | $C_6$ | $C_7$ | $C_8$ | $C_9$ | $C_{10}$ | $C_{11}$ | $C_{12}$ | $C_{13}$ | $C_{14}$ | $C_{15}$ | $C_{16}$ | $C_{17}$ | $C_{18}$ | $C_{19+}$ | | | |
| Palm oil | $NiMoS_2/\gamma$-$Al_2O_3$ | 300°C, $H_2$ 50 bar, LHSV 1 $h^{-1}$ | | | | | | | | | | | | 93.3 % Diesel | | | | | $H_2$ 95%, $C_1$ 1.7%, $C_2$ 0.3%, $C_3$ 2.2%, CO 0.2%, $CO_2$ 0.6% | [14] |
| Algae bio-oil | NiCu/$ZrO_2$ | 350°C $H_2$ 20 bar LHSV 3.5 $h^{-1}$ | | | | | | | | | | | | 91.0 % Diesel | | | | Product were determined by CHN analyzer | A long-term run of 24 h, the HDO efficiency was still larger than 77% and the amount of coke on catalyst was only 2%, indicating that the stability of the bimetallic NiCu | | [26] |
| FAMEs | Ni/HZSM-5 | 280°C $H_2$ 8 bar LHSV 4 $h^{-1}$ | | | 6.8 % Gasoline | | | | | | | | | 27.7 % jet fuel | | 40.6 % Diesel | | | A weight loss of carbon deposition on catalyst approximately 17% was observed by TGA analysis after the catalyst was used for 80 h. The conversion decreased from 85.1% to 30.1% after operation for 80 h | $C_1$-$C_4$ 9%, CO 2%, $CO_2$ 1% | [9] |

| Feed stock | Catalyst | Operating condition | Liquid product yield (%) | | | | | | | | | | | | | | | Product characterization | Catalyst deactivation | Gas product distributions | Ref. |
|---|---|---|---|---|---|---|---|---|---|---|---|---|---|---|---|---|---|---|---|---|---|
| | | | $C_5$ | $C_6$ | $C_7$ | $C_8$ | $C_9$ | $C_{10}$ | $C_{11}$ | $C_{12}$ | $C_{13}$ | $C_{14}$ | $C_{15}$ | $C_{16}$ | $C_{17}$ | $C_{18}$ | $C_{19+}$ | | | | |
| Palm oil | 5Ni/γ-$Al_2O_3$ | 330°C, $H_2$ 50 bar, LHSV 1 $h^{-1}$ | | | | | | | | | | | ← | 26.5 % Diesel | | → | | | | $H_2$ 85%, $C_1$ 13.6%, $C_2$ 0.9%, $C_3$ 0.5%, CO 0%, $CO_2$ 0% | [25] |
| | 5Co/γ-$Al_2O_3$ | | | | | | | | | | | | ← | 94.3 % Diesel | | → | | | | | |
| | 5Pd/γ-$Al_2O_3$ | | | | | | | | | | | | ← | 76.1 % Diesel | | → | | | | | |
| | 5Pt/γ-$Al_2O_3$ | | | | | | | | | | | | ← | 54.0 % Diesel | | → | | | | | |
| Rapeseed oil | NiCu/$ZrO_2$-$CeO_2$ | 300°C, $H_2$ 10 bar, LHSV 2 $h^{-1}$ | | ← | | | 75.0 % liquid hydrocarbon | | | | | | | | | → | | | The results of the tests showed also an intensive coke formation in the case of γ-$Al_2O3$ due to the presence of weak Lewis-type acidic sites on its surface. | | [26] |

# Chapter 4
# Experimental

## 4.1 Material

The PFAD used in this experiment was provided from Patum Vegetable Oil CO., LTD., Thailand and refined palm olein from Morakot Industries PCL., Thailand. HZSM-5 pellet was purchased from Riogen. Inc., USA. TPABr, $Na_2SiO_3$, $Al(NO_3)_3 \bullet 9H_2O$, $Ni(NO_3)_2 \bullet 6H_2O$ and $Cu(NO_3)_2 \bullet 3H_2O$ were purchased from S.M. Chemical CO., LTD., Thailand.

## 4.2 Catalyst preparation

The HZSM-5 (Si/Al molar = 20) was prepared by 0.03 mol of tetrapropyl ammonium bromide (TPABr) as a structure-directing substance dissolved in 50 ml of DI water. 1 mol of sodium silicate and 0.05 mol of aluminium nitrate were dissolved separately in each 20 ml of DI water. Si and Al precursors were added in TPABr solution dropwise under stirring and controlled in the range of pH value of 10.5-10.6 and then, stirred for 30 minute at room temperature. The obtained gel was putted in an autoclave, then heated the mixture to 200°C and held for 24 h. The product was washed with DI water until pH equals to neutral. After that, this powder was dried at 110°C for overnight. Finally, it was calcined under air atmosphere at 550°C.



The obtained NaZSM-5 was further ion-exchanged to achieve HZSM-5 by the following steps: 1 g of NaZSM-5 was stirred with 20 ml of 1 M $NH_4NO_3$ solution for 2 h and then repeated for 3 times. Then, washed with DI water until pH equals 7, dried at 110°C for overnight. Finally, it was calcined under air atmosphere at 550°C for 5 h. The preparation method of NiCu/HZSM-5 catalyst was shown in Fig.4.1.

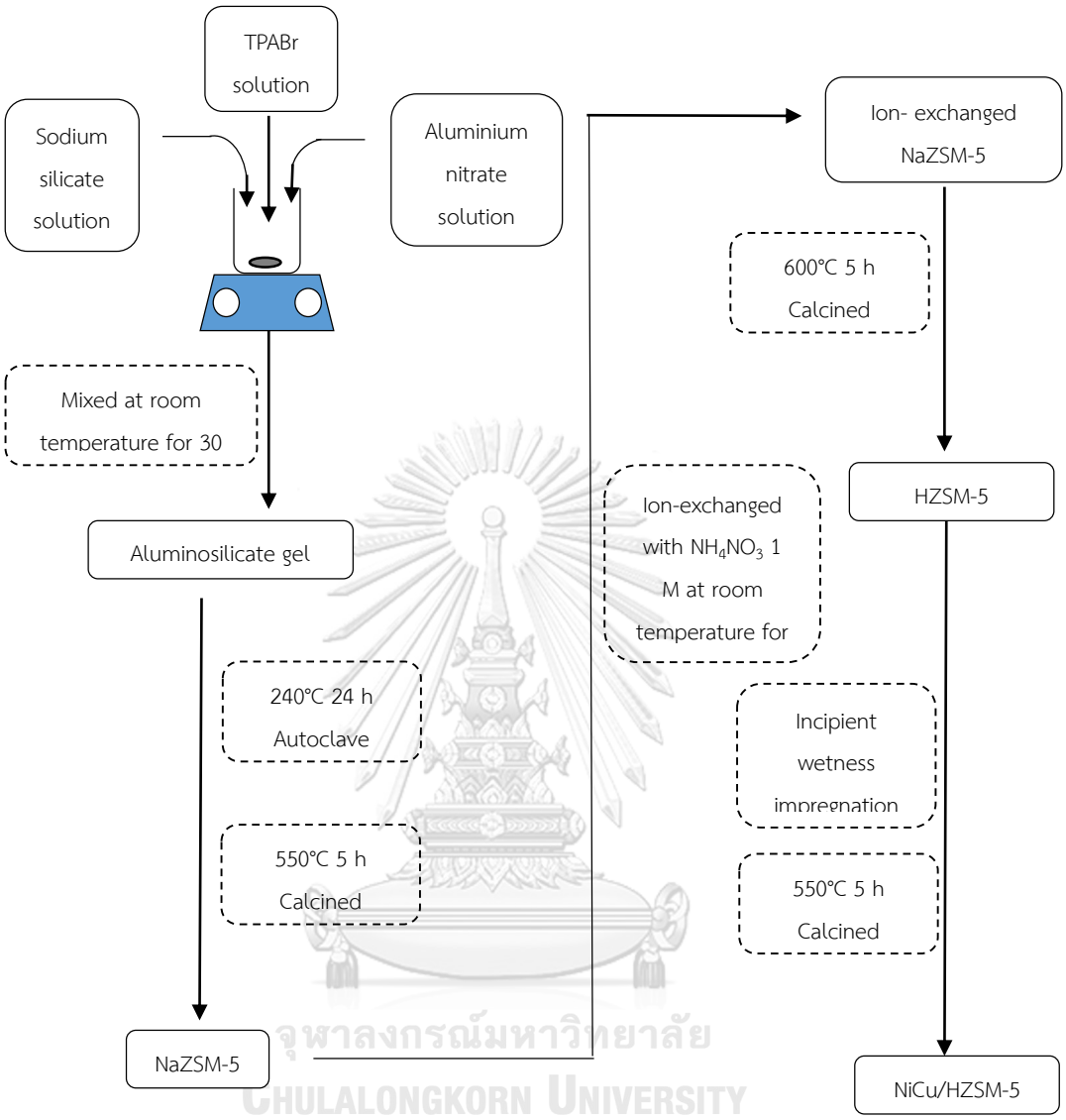




Fig. 4.1 NiCu/HZSM-5 catalyst preparation

For continuous hydroprocessing, commercial pellet HZSM-5 (2.0 mm dimeter) was employed as support. It was dried at 110°C for overnight before use. The HZSM-5 supported NiCu catalyst was prepared by incipient wetness impregnation. Firstly, aqueous solution of $Ni(NO_3)_2{\cdot}6H_2O$ and $Cu(NO_3)_2{\cdot}3H_2O$ were mixed to obtain Cu/Ni mass ratio 12.5Ni2.5Cu wt.%. After that, the mixture of Ni and Cu was dropped on HZSM-5, and was dried by oven at 110°C for overnight to remove moisture. Finally, the resultant substance was calcined at 550°C for 5 h to obtain 12.5Ni2.5Cu/HZSM-5 catalyst.

**4.3 Catalyst characterization**

The crystal structure of catalyst was analyzed by X-ray diffraction (XRD) (Bruker of D8 Advance, 2θ in the range of 5°-80°).

$N_2$ physisorption on BET method was applied to find specific surface area, pore volume and pore diameter of catalyst (using Micromeritics ASAP 2020) at liquid nitrogen temperature of -196°C.

Acidic sites of catalyst were determined by $NH_3$-TPD method (Micromeritics Chemisorb 2750 Pulse Chemisorption System). Firstly, the sample (0.1 g) was prepared into U tube of TPX machine under a He gas flow at ramp rate of 10°C/min to 500°C and held for 30 min. After that, the system was cooled down to 100°C and then ammonia was adsorbed until its saturation for 1 h. Finally, removing excess ammonia under the He gas flow until completely about 1 h and then the system was heated up to 550°C at ramp rate of 10°C/min to desorb ammonia.

Scanning electron microscopy and energy dispersive x-ray spectroscopy (SEM and EDX) were applied to investigate the morphology of catalyst (Hitachi mode S-3400N for SEM while Link Isis series 300 program for EDX).

Coke deposition of used catalyst was determined by thermogravimetric analysis (TGA). The sample was heated up to 1000°C with the ramp rate of 10°C/min.



**4.4 Hydrotreating process**

To find the optimum Cu/Ni ratio in catalyst, 15Ni wt.%, 12.5Ni2.5Cu wt.%, 10Ni5Cu wt.% and 7.5Ni7.5Cu wt.% on HZSM-5 were investigated. The hydrotreating reactions were tested in 100 ml batch reactor with internal diameter of 40 mm and equipped with a mechanical stirrer. The operation limits of reactor were total pressure of 100 bar and 600°C. The catalysts were pre-reduced at reduction temperature of 550°C under hydrogen gas flow rate of 30 ml/min for 2h. Then, the feed consisted of the warmed PFAD (80°C) and the reduced catalyst in a weight ratio of PFAD:catalysts of 30:1. $H_2$ gas was charged into the reactor to the initial pressure of 50 bar. The reactor was then heated up to target temperature (375°C) and the reaction was proceeded for

3 h under stirring speed of 400 rpm. After the reactor was cooled down to room temperature, the gas and liquid products were collected. Fig.4.2 showed the schematic of batch catalytic hydrotreating process for screening catalyst.

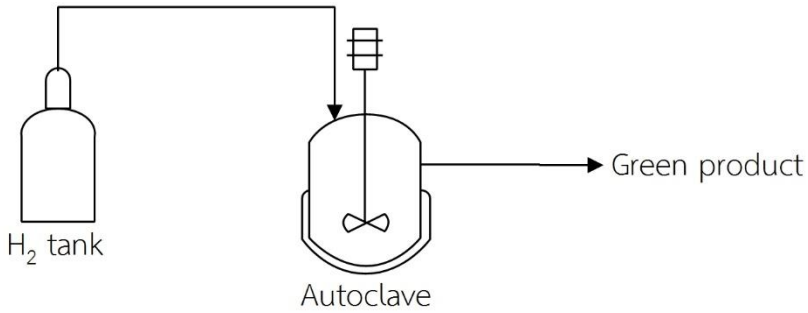


Fig. 4.2 Schematic of batch catalytic hydrotreating process for catalyst screening

Fig.4.3 showed the schematic of continuous catalytic hydrotreating process of palm oil, which was carried out in high-pressure fixed-bed reactor with an internal diameter of 0.952 cm, length of 40 cm and volume of 30 $cm^3$. The catalyst (7.2 g. with a catalyst bed volume of 7 ml) was loaded into a reactor and reduced before start the reaction by heating catalyst to 450°C under $H_2$ gas flow for 2 h. After the system was reduced to the room temperature, palm oil was fed by HPLC feeding pump and mixed with a $H_2$ gas flow in preheater at 100°C. Then, the mixture was introduced into the reactor at 400°C, $H_2$ pressure of 40 bar, LHSV of 1-5 $h^{-1}$. Condenser and gas-liquid separator were used to collect the gas and liquid products.

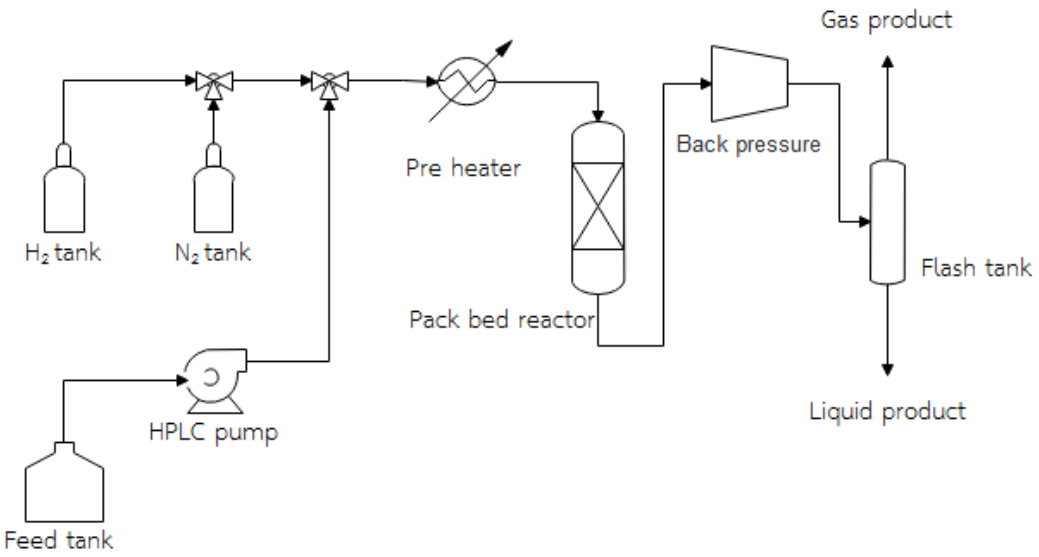


Fig. 4.3 Schematic diagram of continuous catalytic hydrotreating process

### 4.5 Product analysis

The gas products ($H_2$, CO, $CO_2$, $C_1$-$C_4$ alkanes) were analyzed by GC (Shimadzu-14b) equipped with a pack column (Porapax Q, 30 m×0.25 mm), and thermal conductivity detector (TCD). The composition of liquid product was analyzed by GC-FID (Shimadzu-14b) equipped with a capillary column (DB-2887, 30m×0.25 mm) and GC-MS (Shimadzu QP2010) equipped with a capillary column (Rtx-5MS, 30 m×0.25 mm) and MS detector. The conversion of feed, product selectivity and product yield were calculated using the following Equations (1), (2) and (3) respectively [30].



$$\text{Conversion}(\%) = \frac{\text{Feed}_{360+} - \text{Product}_{360+}}{\text{Feed}_{360+}} \times 100 \qquad (1)$$

$$\text{Jet fuel selectivity}(\%) = \frac{\text{Product}_{150-250} - \text{Feed}_{150-250}}{\text{Feed}_{360+} - \text{Product}_{360+}} \times 100 \qquad (2)$$

$$\text{Jet fuel Yield}(\%) = \text{Conversion} \times \text{Selectivityi} \times \text{Liquid fraction} \qquad (3)$$

Here, $Feed_{360+}$ is weight percent of the feed having boiling point higher than 360°C. $Product_{360+}$ is weight percent of the product having boiling point higher than 360°C.

$Feed_{150-250}$ and $Product_{150-250}$ are weight percent of the feed and products, respectively, which have a boiling point between 150 and 250°C (jet fuel molecules).

Moreover, the fraction distillated of boiling point between 65 to 150°C were defined as gasoline range and boiling point between 150 to 360°C were defined as diesel range [30].

# Chapter 5
# Results and discussion

This chapter is divided into two parts. Part 5.1 represented the effect of monometallic catalyst (15Ni wt.%/HZSM-5) and bimetallic catalyst (12.5Ni2.5Cu wt.%, 10Ni5Cu wt.% and 7.5Ni7.5Cu wt.%/HZSM-5) in batch hydrotreating process with autoclave reactor. Part 5.2 illustrated the selected 12.5Ni2.5Cu wt.% loading on commercial pellet-type HZSM-5 catalyst in continuous hydrotreating process.

## 5.1 Effect of different %metal loading catalysts (NiCu/HZSM-5)

### 5.1.1 Catalyst characterization

5.1.1.1 X-ray diffraction (XRD)

XRD patterns of the catalysts are shown in Fig. 5.1. The XRD patterns of HZSM-5 gave a typical pattern of MFI structure (2θ around 23.0°and 23.8° corresponding to the major peak of [303] and [503] crystal plane [37]. The XRD pattern of NiO showed the crystalline pattern as the standard NiO pattern. All diffraction peaks can be well indexed as face-centered cubic phase at 2θ = 37.1°, 43.1°, 62.6°, 75.3° and 79.1° which are assignable to [111], [200], [220], [311] and [222] crystal planes, respectively. [38] The XRD diffraction peaks of all Cu-loading catalysts exhibited at 2θ = 37.1° and 43.1° which are assignable to [111] and [220] crystal planes [38].

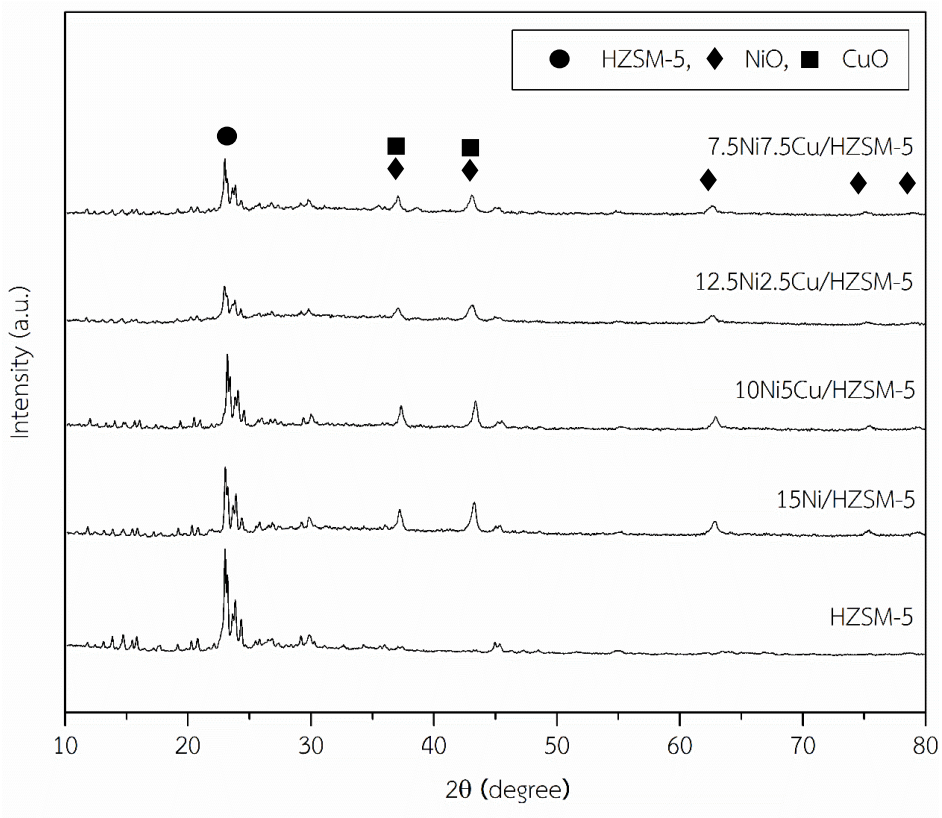


Fig. 5.1 The XRD patterns of monometallic (15Ni wt.%.) and bimetallic (12.5Ni2.5Cu wt.%, 10Ni5Cu wt.% and 7.5Ni7.5Cu wt.%) on HZSM-5 supported catalyst.



5.1.1.2 Ammonia temperature programmed desorption ($NH_3$-TPD)

Ammonia temperature programmed desorption ($NH_3$-TPD) is a common technique to determine the acidity on the surface of catalysts. The strong and weak acidities were related to the desorption temperature. Moreover, the total amount of ammonia desorption was considered to correspond with the amount of total acidity at surface of catalysts [9].

**Table 5.1** Acidity from $NH_3$-TPD of NiCu/HZSM-5 catalysts

| Samples | Acid density (mmol $H^+$/g cat) | | Total acid site |
|---|---|---|---|
| | Weak acid site | Strong acid site | |
| HZSM-5 | 0.92 | 1.04 | 1.96 |
| 15Ni/HZSM-5 | 1.28 | 0.61 | 1.89 |
| 12.5Ni2.5Cu/HZSM-5 | 1.28 | 0.80 | 2.07 |
| 10Ni5Cu/HZSM-5 | 1.19 | 0.80 | 2.00 |
| 7.5Ni7.5Cu/HZSM-5 | 1.11 | 0.88 | 1.98 |

$NH_3$-TPD profiles of catalysts were determined in the temperature range of 100-800°C. According to Fig.5.2, the two maximum desorption peaks for each catalyst were shown in TPD curves. The peak at high temperature was denoted as strong acid site, whereas another peak at low temperature was assigned to weak acid site [39]. These desorption peaks were de-convoluted and summarized to obtain the amount of weak and strong acid densities as reported in Table 5.1. For HZSM-5 supported catalyst, two distinct desorption peaks of $NH_3$ appeared about 240°C and 435°C. The desorption peak at low temperature was defined as weak acid while the peak centered at high temperature was defined as strong acid [39]. After Ni and Cu loading, the peak position of weak and strong acidic sites shifted to higher temperature which caused by Brønsted and Lewis acid sites. From the research reported that the Lewis acid sites could originate from the high dispersion of copper species at high temperature [40]. In addition, the strong acid was decreased while weak acid was increased after Ni and NiCu was added due to Brønsted acid protons of $Ni^{2+}$ and $Cu^{2+}$ [9, 40]. The total acid sites of NiCu/HZSM-5 catalysts were in the range of 1.89-2.07 mmol $H^+$/g. cat.

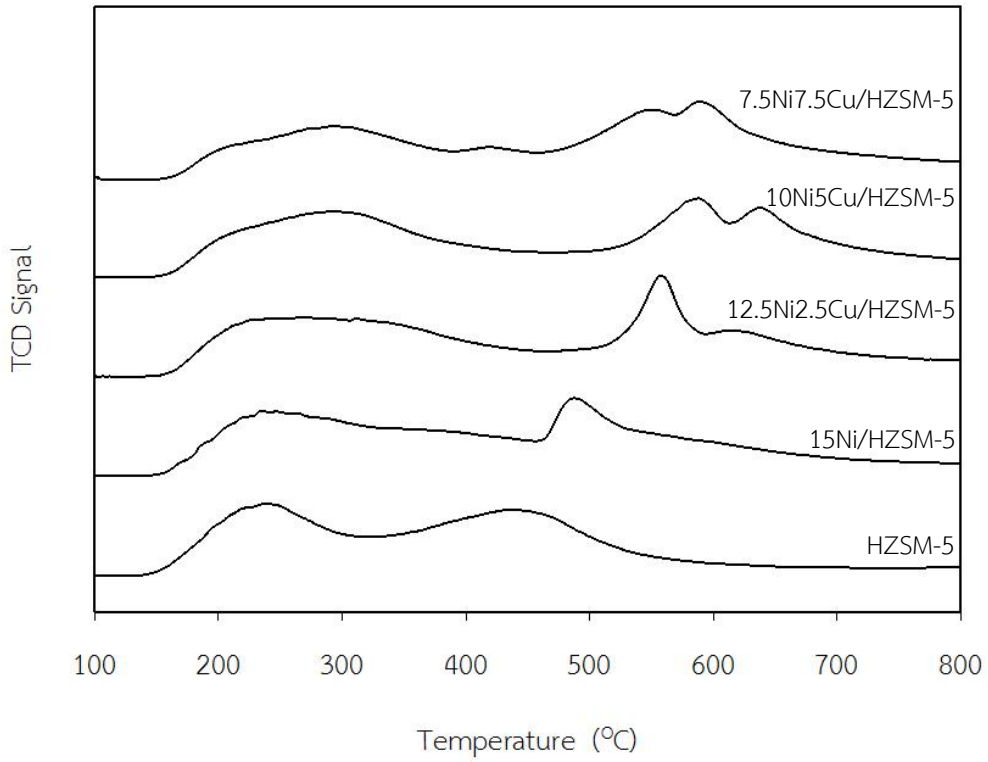


Fig. 5.2 $NH_3$-TPD profiles of NiCu/HZSM-5 with different Cu/Ni ratios.

5.1.1.3 Hydrogen temperature programmed reduction ($H_2$-TPR)

$H_2$-TPR was applied to investigate the activation temperature of NiCu/HZSM-5 catalyst for HDO reaction. The $H_2$-TPR profile of catalysts were given in Fig. 5.3. The 15wt.%Ni/HZSM-5 revealed a significant peak at temperature approx. 400°C, which was attributed to the reduction of NiO. The reduction peak between 230°C and 300°C was likely associated with the reduction of $Cu^{2+}$ to $Cu^0$ [26]. The peaks higher than 300°C were associated the reaction of bimetallic NiCu species [41] and the reduction of $Ni^{2+}$ to $Ni^0$ [26]. As reported by TPR curve of NiCu/HZSM-5 catalysts, the reduction peaks shifted to a low temperature (centered at approximately 340°C for 12.5Ni2.5Cu, 285°C for 10Ni5Cu and 240°C for 7.5Ni7.5Cu on HZSM-5 supported catalyst, respectively) compared with 15Ni/HZSM-5. As a consequence, NiCu/HZSM-5 catalyst was conducted. The result revealed that it could promote the metal oxide reduction. This was because temperature reduction was dropped after Cu was added on Ni/HZSM-5 catalyst [28]. This observation recommended that the Gibbs free energy of

reduction of bimetallic NiCu sample was lower for this oxide (−100.65 kJ/mol at 25°C) than for NiO (−12.31 kJ/mol at 25°C) [42].

Furthermore, Table 5.2 summarized the reducing temperature and the amount of oxygen atoms removed which were measured by $H_2$-TPR analysis with different Cu/Ni ratios. NiCu/HZSM-5 displayed the amounts of oxygen atoms which were removed in the range of 0.02-0.04 mmol/g.

**Table 5.2** Reducing temperature and amount of oxygen atoms removed

| Samples | $T_{max}$ (°C) | Oxygen atoms removed | |
|---|---|---|---|
| | | ($\times10^{-3}$ mol/g) | ($\times10^{21}$ atom/g) |
| 15Ni/HZSM-5 | 430 | 0.04 | $2.53\times10^{22}$ |
| 12.5Ni2.5Cu/HZSM-5 | 380 | 0.03 | $1.98\times10^{22}$ |
| 10Ni5Cu/HZSM-5 | 340 | 0.03 | $1.79\times10^{22}$ |
| 7.5Ni7.5Cu/HZSM-5 | 320 | 0.02 | $1.95\times10^{22}$ |

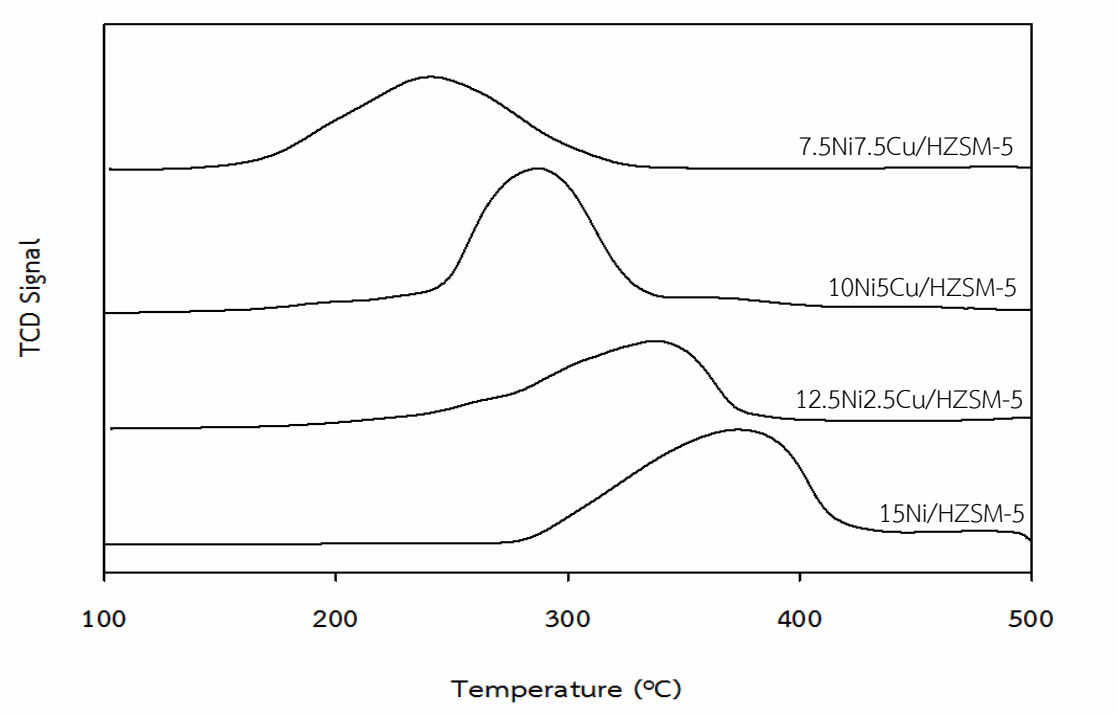


Fig. 5.3 $H_2$-TPR profiles of NiCu/HZSM-5 with different Cu/Ni ratios.

5.1.1.4 Scanning electron microscopy analyses and energy dispersive x-ray spectroscopy (SEM-EDX)

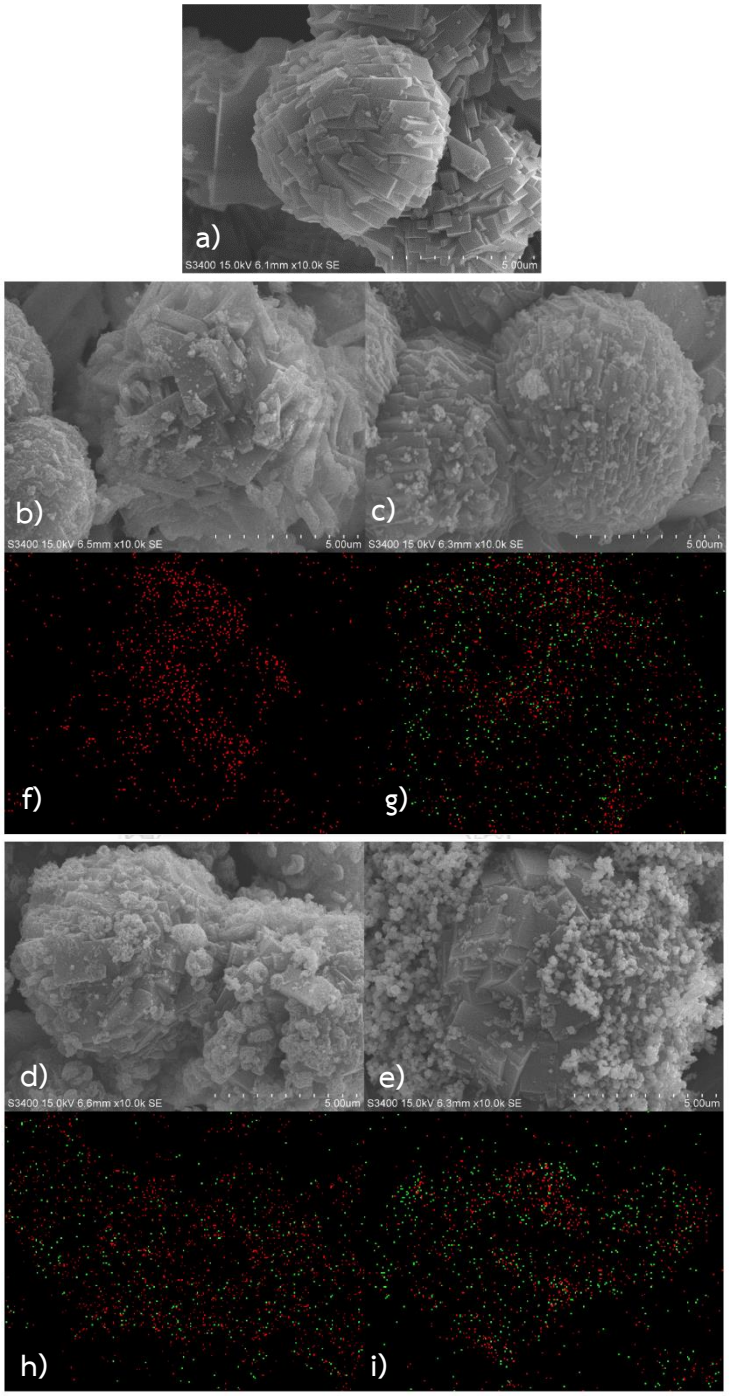


Fig. 5.4 SEM-EDX images of NiCu/HZSM-5 with different Cu/Ni ratios

(red points are NiO and green points are CuO)

From Fig.5.4a-5.4e, SEM images (a. HZSM-5, b. 15Ni/HZSM-5, c. 12.5Ni2.5Cu/HZSM-5, d. 10Ni5Cu/HZSM-5, e. 7.5Ni7.5Cu/HZSM-5), indicated the similar particle size (approximate 5 μm) and had hexagonal cubic morphology. According to Fig.5.4f-5.4i, EDX mapping images of catalysts, which are f. 15Ni/HZSM-5, g. 12.5Ni2.5Cu/HZSM-5, h. 10Ni5Cu/HZSM-5, i. 7.5Ni7.5Cu/HZSM-5, showed well dispersed of Ni and Cu on catalyst surface. Furthermore, the percent weight of metal on the catalyst surface measured by EDX technique was according with the percent weight of loaded metal.

5.1.1.5 $N_2$-physisorption

The physical structure properties of NiCu/HZSM-5 catalysts were shown in Table 5.3. Bare HZSM-5 support had BET surface area of 332.1 $m^2/g$. After impregnation with Ni and NiCu, the BET surface area decreased to 263.45 $m^2/g$ for 15Ni/HZSM-5 and 232.11-262.99 $m^2/g$ for NiCu/HZSM-5 with different Cu/Ni loading ratios. In this case, it could be explained by the SEM images in Fig.5.4 that they showed well dispersed of Ni and Cu particles on catalyst surface but the added Ni and NiCu might block the channels of HZSM-5 catalyst surface, leading to decrease in surface area and increase in pore size [43, 44]. In addition, the pore sizes of catalysts were in the range of 21.2 to 27.8 $A^o$ which are macro sizes.

**Table 5.3** BET surface areas, pore volume and pore size of NiCu/HZSM-5 catalysts

| Catalyst | BET Surface area ($m^2/g$) | Pore Volume ($cm^3/g$) | Pore Size ($A^o$) |
|---|---|---|---|
| HZSM-5 | 332.15 | 0.178 | 21.4 |
| 15Ni | 263.45 | 0.183 | 27.8 |
| 12.5Ni2.5Cu | 238.45 | 0.133 | 22.3 |
| 10Ni5Cu | 232.11 | 0.150 | 25.4 |
| 7.5Ni7.5Cu | 262.99 | 0.139 | 21.2 |

Determined by $N_2$ physisorption

### 5.1.2 Catalyst hydroprocessing

5.1.2.1 Effect of catalysts

Fig. 5.5 shows the effect of different Ni and Cu loading on PFAD conversion and selectivity of the liquid product. under the reaction conditions temperature of 375℃, $H_2$ pressure of 50 bar and 3 h of reaction time. The product yield is displayed in Fig. 5.6 and summarized in Table 5.4. Comparing to HZSM-5, doping with 15wt% Ni provided slightly PFAD conversion; however, selectivity of diesel decreased with increasing of gasoline selectivity. This is because Ni could promote cracking of Ni-$H_2$ bond activity for 15Ni/HZSM-5. In addition, the added 2.5wt.%Cu on HZSM-5 could improve the activity of Ni due to $H_2$ spillover. However, the excess amount of Cu loading (5wt.%, 7.5wt%) caused the reduction of Ni activity because the content of Ni on catalyst decreased and Cu might be block active site [45].

As a result, 12.5Ni2.5Cu/HZSM-5 provided the highest conversion and jet fuel yield of 94.79% and 39.27%, respectively. In detail, each hydrogen molecule could easily adsorb on Ni surfaces than Cu surfaces because Cu had higher biding energies of hydrogen bond than Ni. In addition, the large difference of the binding energies of hydrogen bound to Ni and Cu makes the spillover of hydrogen from Ni to Cu energetically unpreferred. Therefore, the hydrogen atoms on Ni sites could be supplemented from gas phase hydrogen after the hydrogen atoms spillover from Ni to Cu which promoting hydrogenation reaction. Moreover, the spillover of hydrogen from Ni to Cu could be promoted by increasing the chemical potential of hydrogen on Ni, which could be achieved by increasing hydrogen adsorption pressure and temperature, or weakening the interaction between Ni and hydrogen [28]. However, the further increase of Cu in excess on catalyst had affect to active hydrogen would be too weak because the Cu block the Ni on surface catalysts [19].

**Table 5.4** Effect of catalysts on liquid products

| Catalyst | Conversion (%) | Liquid fraction | Selectivity (%) | | | Yield (%) | | |
|---|---|---|---|---|---|---|---|---|
| | | | Gasoline | Bio jet | Green diesel | Gasoline | Bio jet | Green diesel |
| HZSM-5 | 76.75 | 0.70 | 23.41 | 43.35 | 33.24 | 12.58 | 23.29 | 17.86 |
| 15Ni/HZSM-5 | 78.49 | 0.74 | 28.90 | 43.27 | 27.83 | 16.78 | 25.13 | 16.17 |
| 12.5Ni2.5Cu/HZSM-5 | 94.79 | 0.83 | 36.90 | 49.92 | 13.18 | 29.03 | 39.27 | 10.37 |
| 10Ni5Cu/HZSM-5 | 67.86 | 0.86 | 14.98 | 44.97 | 40.05 | 8.75 | 26.24 | 23.38 |
| 7.5Ni7.5Cu/HZSM-5 | 65.98 | 0.86 | 19.48 | 44.96 | 35.56 | 11.05 | 25.51 | 20.17 |

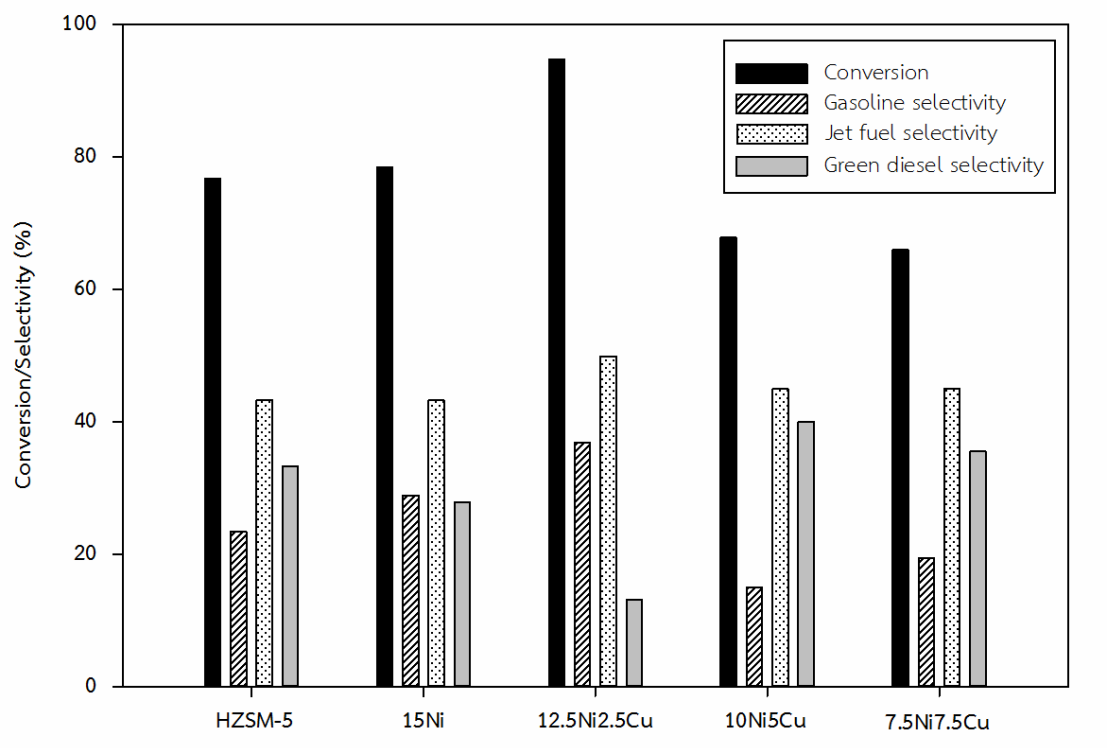


Fig. 5.5 Effect of catalysts on conversion and selectivity from the liquid product in batch reactor (Temperature of 375°C, $H_2$ pressure of 50 bar, reaction time of 3 h., catalyst of 1 g. and PFAD of 30 g.).

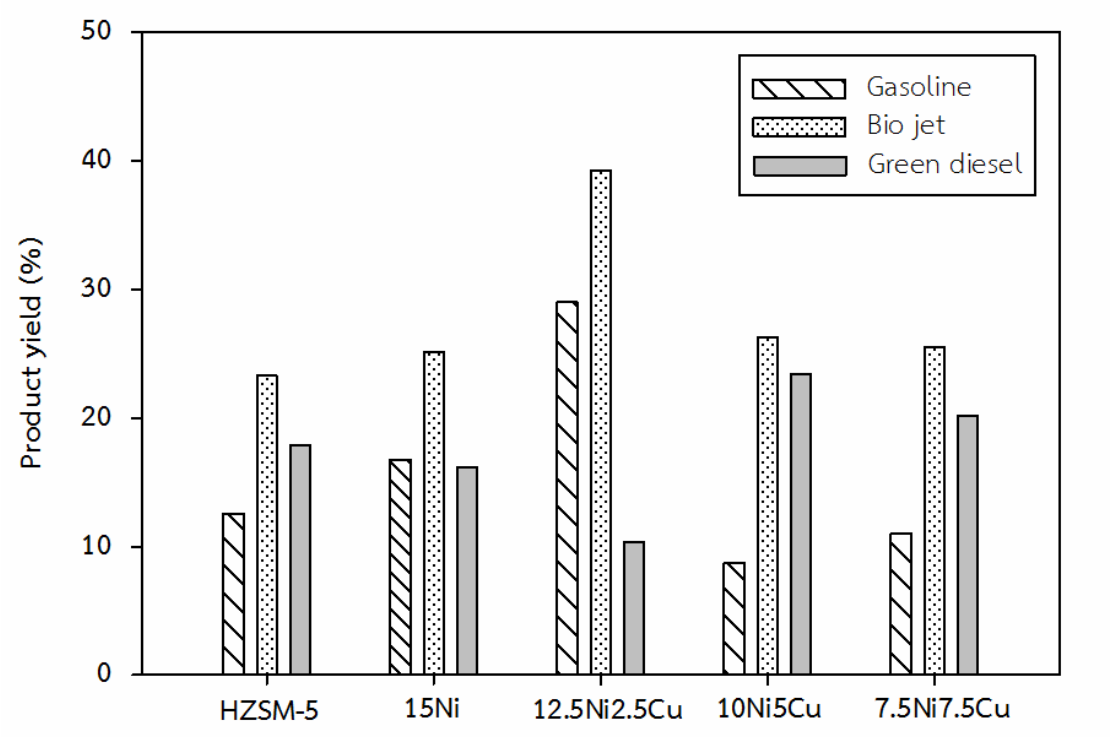


Fig. 5.6 Effect of catalysts on product yield

**Table 5.5** Compositions of liquid product by GC-MS analysis (vol.%)

| Composition | HZSM-5 | 15Ni/HZSM-5 | 12.5Ni2.5Cu/HZSM-5 |
|---|---|---|---|
| N-alkane | 36.70 | 34.82 | 27.67 |
| Iso-alkane | 49.05 | 47.87 | 48.74 |
| Alicyclic | 2.92 | 4.08 | 5.52 |
| Alkylbenzene | 5.73 | 7.24 | 10.36 |
| Toluene | 2.66 | 2.12 | 3.60 |
| Alkene | 2.12 | 2.84 | 2.63 |
| Alkyne | 0.81 | 1.01 | 1.47 |
| Iso/Normal ratio | 1.34 | 1.37 | 1.76 |
| Aromatic | 8.39 | 9.38 | 13.96 |

Table 5.5 shows the composition of liquid products which were n-alkane, iso-alkane, alicyclic, alkybenzene, toluene, alkene, alkyne, iso/normal ratio and aromatic. HZSM-5 and 15Ni/HZSM-5 had a similar iso/normal ratio and aromatic content. The 12.5Ni2.5Cu/HZSM-5 exhibited the highest iso/normal ratio of 1.76 and aromatic content of 13.96 vol.%. High isomerization and aromatization product is preferred for jet fuel because the better cold flow property and heat of combustion. From this result, it could be said that doping with 2.5% Cu (12.5Ni2.5Cu/HZSM-5) could improve the isomerization and aromatization reaction which might be the fact that hydrogen was saturated on surface area of catalyst by hydrogen spillover.

5.1.2.2 Deactivation of catalysts

Fig. 5.7 shows the TGA analysis of spent catalysts at 40-1000°C. The weight loss at the temperature lower than 200°C was approximate 3% for all catalysts which should be corresponding to the amount of water desorption while the temperature between 200-420°C was a volatile substance. The weight loss of carbon was depended on temperature between 420-670°C. From this figure, HZSM-5 promoted the highest amount of coke formation ca. 8 wt.%. 15Ni/HZSM-5 had amount of coke formation ca. 7 wt.%. Although 12.5Ni2.5Cu/HZSM-5 exhibited much higher activity, 12.5Ni2.5Cu/HZSM-5 showed amount of coke formation approx. 5 wt.%. which was similar to that of 10Ni5Cu/HZSM-5 and slightly higher than 7.5Ni7.5Cu/HZSM-5. This might be due to the fact that the hydrogen spillover of active hydrogen was saturated on surface area when Cu was added and therefore preventing coke formation [26].

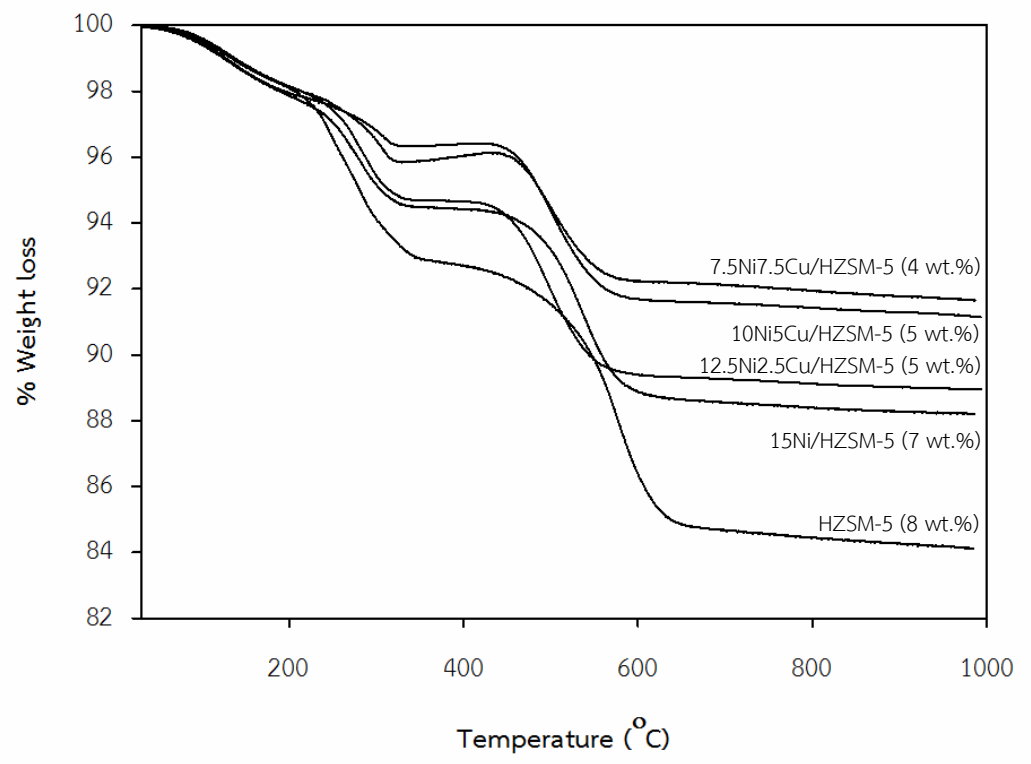


Fig. 5.7 TG analysis of the catalysts

## 5.2 Effect of NiCu/HZSM-5 in continuous hydrotreating process

### 5.2.1 Catalyst characterization

5.2.1.1 X-ray diffraction (XRD)

XRD patterns of HZSM-5 powder and commercial pellet-type HZSM-5 were shown in Fig. 5.8. They exhibited a typical pattern of MFI structure (2θ around 23.0°and 23.8° corresponding to the major peak of [303] and [503] crystal planes, respectively [37]. Fig. 5.9 showed the XRD pattern of 12.5Ni2.5Cu/HZSM-5 powder compared with the commercial pellet-type. The XRD pattern of NiO showed the crystalline pattern as the standard NiO pattern. The diffraction peaks can be well indexed as face-centered cubic phase at 2θ = 37.1°, 43.1°, 62.6°, 75.3° and 79.1° which are assignable to [111], [200], [220], [311], and [222] crystal planes, respectively [38]. The XRD diffraction peaks of all Cu-loading catalysts exhibited at 2θ = 37.1° and 43.1° which are assignable to [111] and [220] crystal planes, respectively [38].

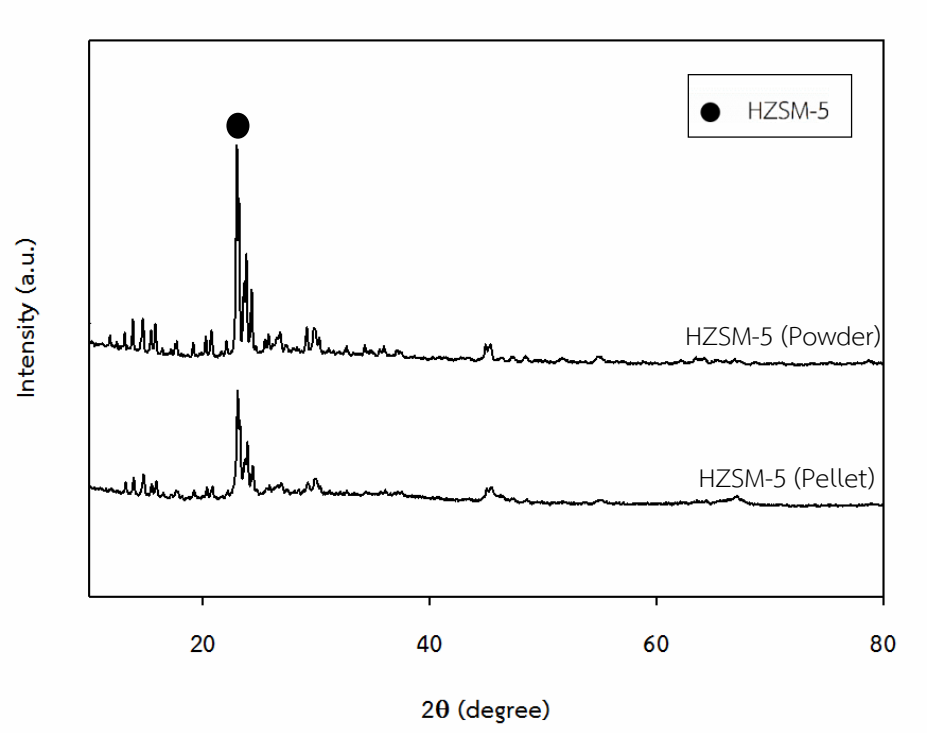


Fig. 5.8 The XRD patterns of HZSM-5 in-house synthesized powder and commercial pellet-type catalyst

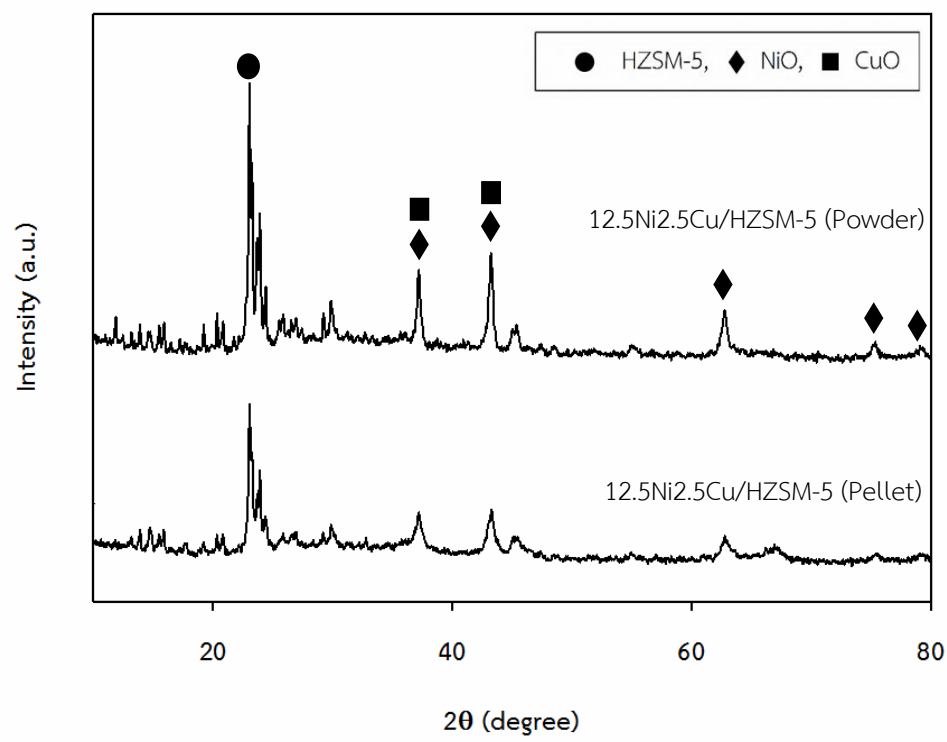


Fig. 5.9 The XRD patterns of 12.5Ni2.5Cu/HZSM-5 powder and commercial pellet-type catalyst

5.2.1.2 Ammonia temperature programmed desorption ($NH_3$-TPD)

$NH_3$-TPD profiles of catalysts were recorded in the temperature range of 100-800°C. $NH_3$-TPD profile of 12.5Ni2.5Cu/HZSM-5 powder and commercial pellet-type were shown in Fig. 5.10. As summarized in Table 5.6, the total acid density of commercial pellet-type HZSM-5 catalyst was lower than that of powder catalyst. This was because commercial pellet-type catalyst had Si/Al ratio of 25 whereas the in-house synthesized powder catalyst had Si/Al ratio of 20.

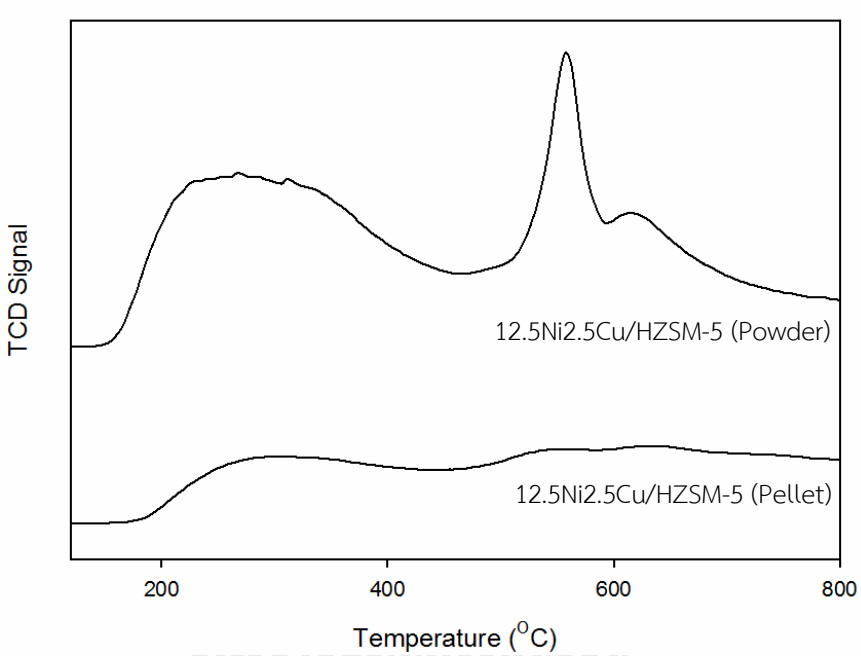




Fig. 5.10 $NH_3$-TPD profiles of 12.5Ni2.5Cu/HZSM-5 commercial pellet-type catalyst

**Table 5.6** Acidity from $NH_3$-TPD of 12.5Ni2.5Cu/HZSM-5 catalysts powder and commercial pellet-type

| Samples | Acid density (mmol $H^+$/g cat) | | Total acid site |
|---|---|---|---|
| | Weak acid site | Strong acid site | |
| 12.5Ni2.5Cu/HZSM-5 (Powder) | 1.28 | 0.80 | 2.08 |
| 12.5Ni2.5Cu/HZSM-5 (Pellet) | 0.67 | 0.57 | 1.24 |

5.2.1.3 Hydrogen temperature programmed reduction ($H_2$-TPR)

The report in Fig. 5.11 by TPR curve of commercial pellet-type HZSM-5 catalyst, the reduction peaks of NiO and CuO shifted to a higher temperature compared with that of powder catalyst. In addition, the high reduced temperature by $H_2$-TPR analysis of commercial pellet-type HZSM-5 catalyst was found at 430 °C.

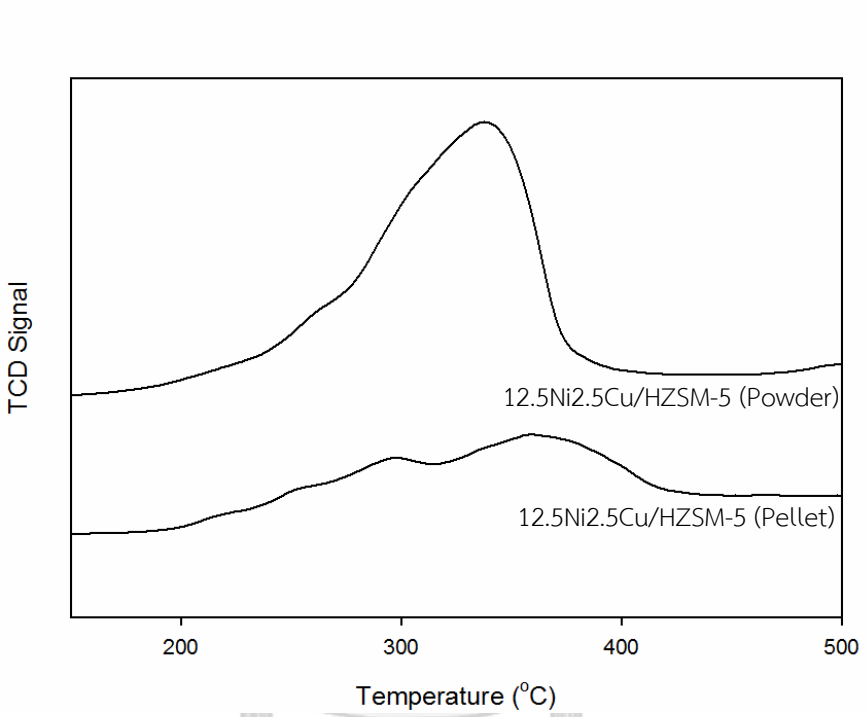


Fig. 5.11 $H_2$-TPR profiles of 12.5Ni2.5Cu/HZSM-5 commercial pellet-type catalyst



5.2.1.4 Scanning electron microscopy analyses and energy dispersive x-ray spectroscopy (SEM-EDX)

From Fig.5.12a-5.12c, SEM images of 12.5Ni2.5Cu/HZSM-5 indicated the similar particle size (approximate 2 μm). According to Fig.5.12d, EDX mapping images of catalyst showed well dispersed of Ni and Cu on catalyst surface. Furthermore, from the result of EDX, it was found that percent weight of metal on catalyst surface was similar to the calculated metal loading.

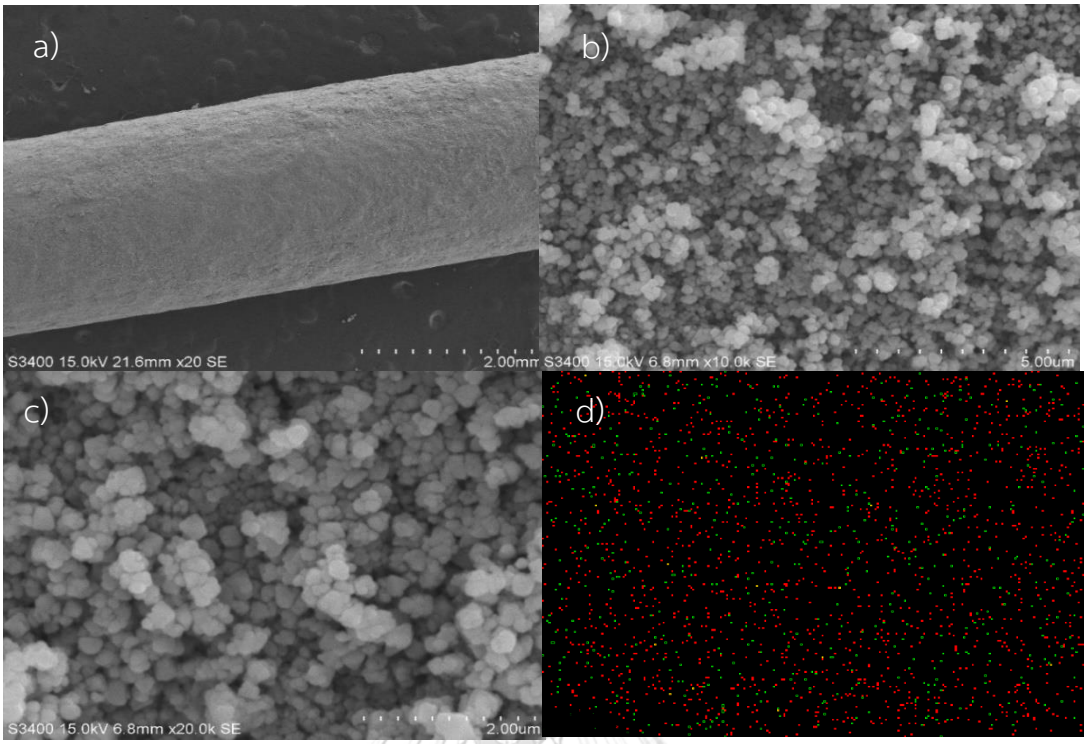


Fig. 5.12 SEM-EDX images of 12.5Ni2.5Cu/HZSM-5 commercial pellet-type catalyst (red points are NiO and green points are CuO)

5.1.1.5 $N_2$-physisorption

The physical structure properties of NiCu/HZSM-5 catalysts were shown in Table 5.7. Pellet-type HZSM-5 had BET surface area of 328.1 $m^2/g$. After impregnation with 12.5%Ni and 2.5%Cu, the BET surface area decreased to 246.4 $m^2/g$. In addition, the pore size of catalysts was in the range of 36.4 to 38.5 $A^\circ$ which was bigger than the pore size of HZSM-5 powder.

**Table 5.7** BET surface areas, pore volume and pore size of NiCu/HZSM-5 powder and commercial pellet-type

| Catalyst | BET Surface area ($m^2/g$) | Pore Volume ($cm^3/g$) | Pore Size ($A^o$) |
|---|---|---|---|
| HZSM-5 (Powder) | 332.1 | 0.178 | 21.4 |
| 12.5Ni2.5Cu/HZSM-5 (Powder) | 238.4 | 0.133 | 22.3 |
| HZSM-5 (Pellet) | 328.1 | 0.316 | 38.5 |
| 12.5Ni2.5Cu (Pellet) | 246.4 | 0.224 | 36.4 |

### 5.2.2 Catalyst hydroprocessing

5.2.2.1 Effect of LHSV

Fig. 5.13-5.14 showe the effect of LHSV on hydroprocessing performance (conversion, selectivity and product yield) under the reaction conditions of 400℃, 40 bar and reaction time 4 h. As summarized in Table 5.8, the catalysts had similar liquid fraction of 0.75 LHSV at 1 $h^{-1}$. Conversion decreased from 96.07% to 90.1 and 46.61% when increased LHSV from 1 to 2 and 5 $h^{-1}$. Similar tendency of jet yield as a function of LHSV can be observed. This result could be explained by the fact that lower LHSV, lower residence time for deoxygenation and cracking. However, at LHSV of 1 $h^{-1}$, the flow of liquid product was not smooth and steady state operation is difficult to reach.



**Table 5.8** Effect of LHSV on liquid products

| LHSV ($h^{-1}$) | Conversion (%) | Liquid fraction | Selectivity (%) | | | Yield (%) | | |
|---|---|---|---|---|---|---|---|---|
| | | | Gasoline | Bio jet | Green diesel | Gasoline | Bio jet | Green diesel |
| 1 | 96.07 | 0.75 | 22.02 | 71.09 | 6.89 | 15.87 | 51.22 | 4.96 |
| 2 | 90.10 | 0.75 | 28.69 | 62.46 | 8.56 | 18.63 | 40.56 | 5.74 |
| 5 | 46.41 | 0.75 | 27.17 | 49.80 | 23.03 | 9.46 | 17.34 | 8.02 |

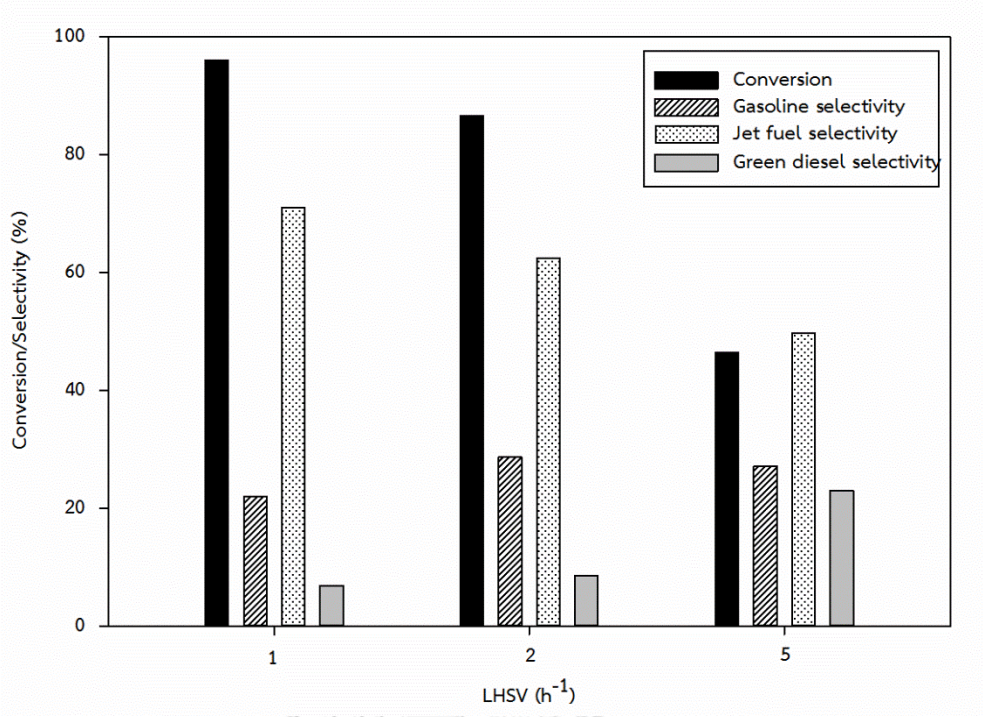


Fig. 5.13 Effect of LHSV on a conversion of palm oil and selectivity for liquid product

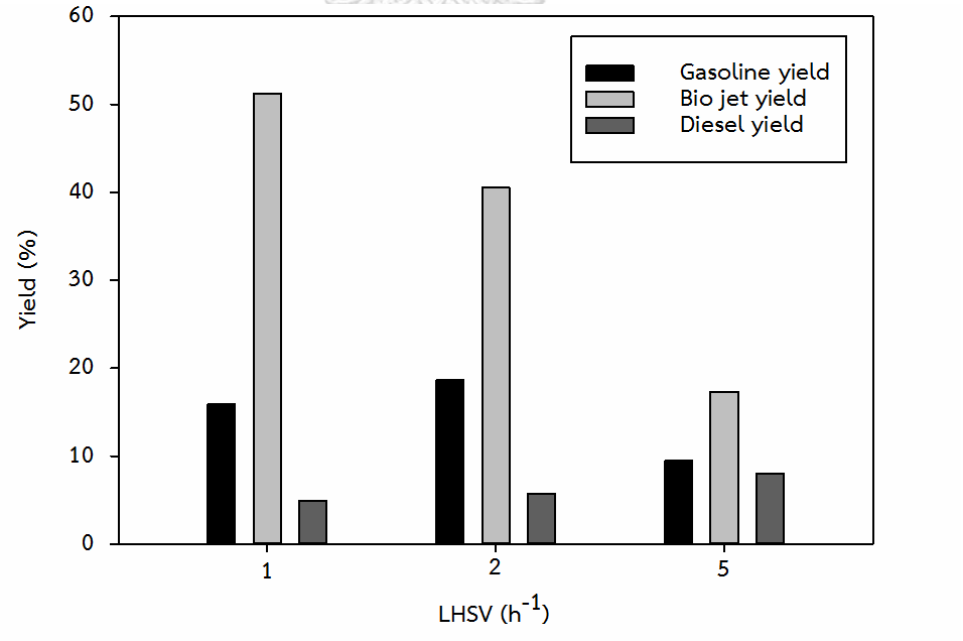


Fig. 5.14 Effect of LHSV on a yield for liquid product

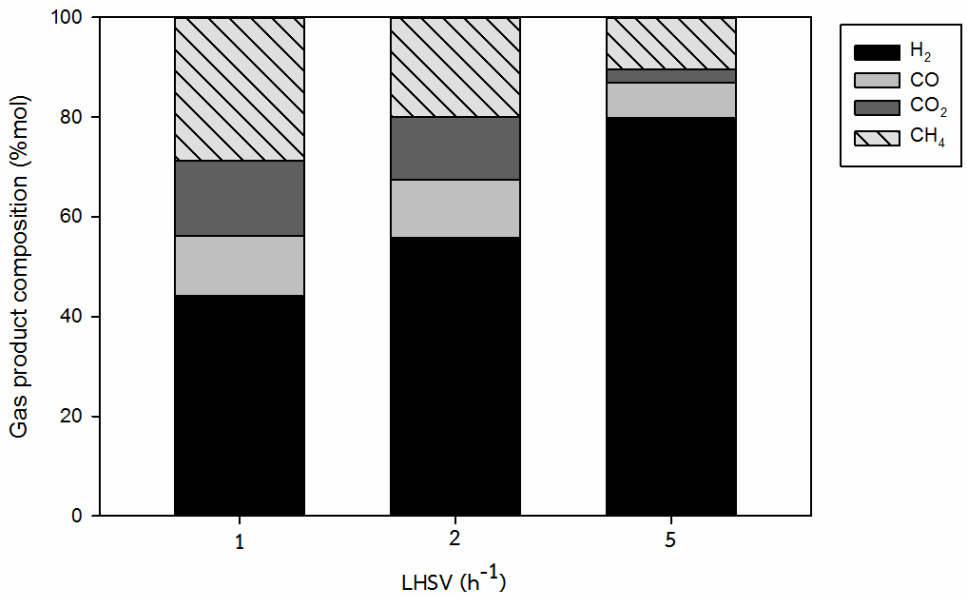


Fig. 5.15 Effect of LHSV on a gas product composition

Gas product composition including $H_2$, CO, $CO_2$ and $CH_4$ are shown in Fig. 5.15. It is worth to note that due to the presence of CO, $CO_2$, water and hydrogen, the reactions such as water gas shift and methanation could also take place. Therefore, identifying the reaction between decarboxylation and decarbonylation is difficult. However, it is obvious that the fraction of $H_2$ decreased with decreasing LHSV because $H_2$ consumption from deoxygenation and cracking reaction. Moreover, $H_2$ consumption by methanation was more pronounced with lower LHSV as indicating by high fraction of methane.

**Table 5.9** Composition of liquid product (before distillation) and bio jet range product (after distillation) of 12.5Ni2.5Cu/HZSM-5 pellet by GC-MS analysis (vol.%)

| Composition | Liquid product | Bio jet fuel |
|---|---|---|
| N-alkane | 19.61 | 25.77 |
| Iso-alkane | 33.97 | 49.53 |
| Alicyclic | 4.75 | 2.47 |
| Alkylbenzene | 26.87 | 22.02 |
| Toluene | 11.85 | - |
| Alkene | 1.02 | 0.20 |
| Alkyne | 1.94 | - |
| Iso/Normal ratio | 1.73 | 1.92 |
| Aromatic | 38.72 | 22.02 |

Table 5.9 shows the composition of liquid product (before distillation) and bio jet range product (after distillation) of 12.5Ni2.5Cu/HZSM-5 commercial pellet-type which were n-alkane, iso-alkane, alicyclic, alkybenzene, toluene, alkene, alkyne, iso/normal ratio and aromatic. Liquid product had iso/normal ratio and aromatic of 1.73 and 38.72 vol.%, respectively. After liquid product was distilled to bio jet fuel, iso/normal ratio increased to 1.92 because iso-alkane compositions were mainly found in jet range ($C_9$-$C_{14}$) while aromatic volume decreased to 22.02 because some aromatics were in the range of light hydrocarbon ($C_5$-$C_8$) such as toluene, methylbenzene. From this result, iso/normal ratio was similar with hydrotreating process in batch reactor (12.5Ni2.5Cu/HZSM-5 powder catalyst). Furthermore, Table 5.10 showed the net heat of combustion and aromatic volume at 42.29 MJ/kg and 24.49%, respectively which comply to ASTM D 1655 and ASTM D 7566.



**Table 5.10** Quality of bio jet fuel compared with ASTM D 1655 and ASTM D 7566

| Property | | D 1655 | D 7566 | Bio jet fuel |
|---|---|---|---|---|
| Net heat of combustion (MJ/kg) | min | 42.8 | 42.8 | 42.92 |
| Aromatic, vol. % | max | 25 | 25 | 22.02 |

5.2.2.2 Stability and deactivation of catalyst

To investigate the catalyst stability, 12.5Ni2.5Cu/HZSM-5 was used continuously for the the catalytic hydroprocessing of palm oil at 400°C, $H_2$ pressure of 40 bar, LHSV of 2 $h^{-1}$ and $H_2$/oil molar ratio of 100. As shown in Fig. 5.16, high catalyst stability is observed over 36 h; however, conversion decreased from 90.09% to 36.50% after the operation time of 103 h. Comparing to research used 10Ni/HZSM (Si/Al = 25) and operation conditions at lower temperature of 280°C, $H_2$ pressure of 40 bar, LHSV of 1 $h^{-1}$ and $H_2$/oil molar ratio of 15 in catalytic hydroprocessing of FAME aiming to produce diesel. They revealed that conversion decreased from 85% to 30% within 80 h [9].

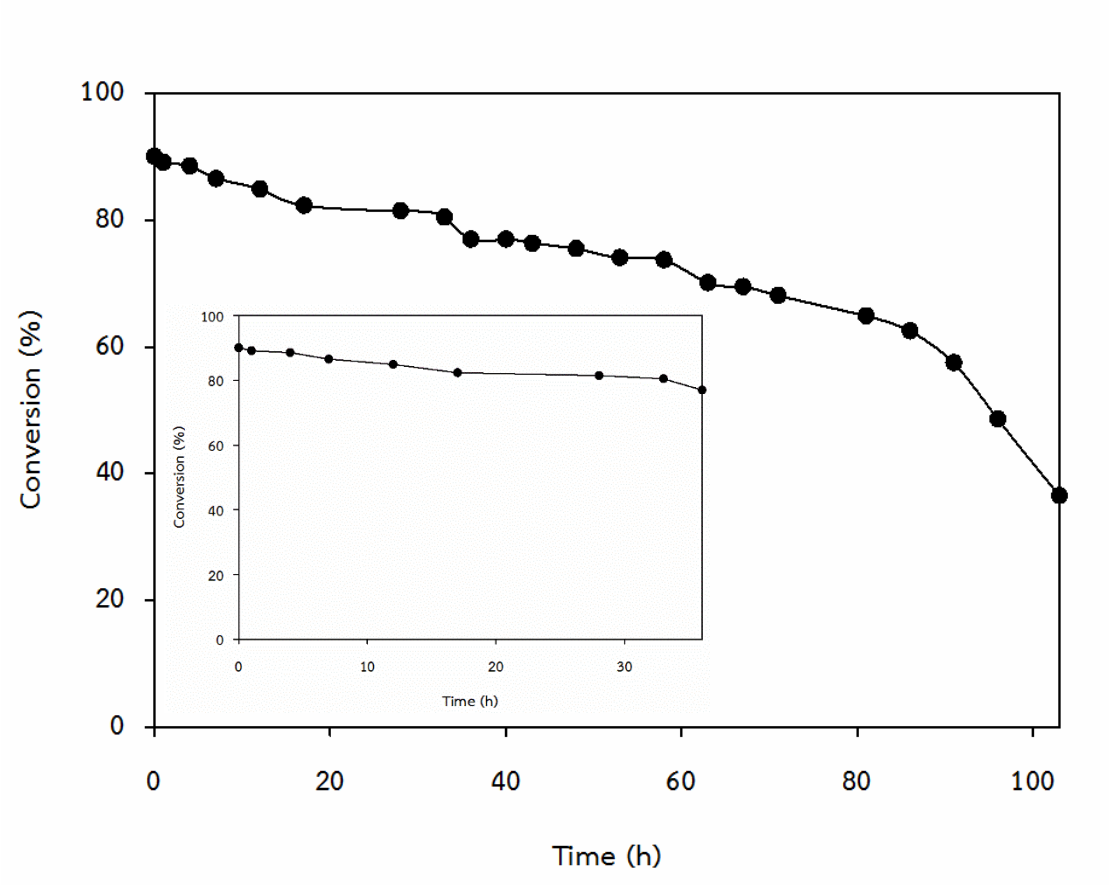


Fig. 5.16 Stability of 12.5Ni2.5Cu/HZSM-5 in catalytic hydroprocessing

# Chapter 6 Conclusions and recommendation

## 6.1 Conclusions

In this study, the bimetallic NiCu/HZSM-5 catalysts were prepared by incipient wetness impregnation. The physicochemical properties of catalysts were investigated by XRD, $NH_3$-TPD, $H_2$-TPR, SEM-EDX, $N_2$-physisorption. The different loadings of Cu/Ni mass ratio of the catalyst were studied in batch reactor for catalyst screening. At the operating temperature of 375°C, initial $H_2$ pressure of 50 bar and reaction time of 3 h, 12.5Ni2.5Cu/HZSM-5 exhibited the highest PFAD conversion of 94.79% and provided a highest bio jet yield of 39.27%. The 12.5Ni2.5Cu/HZSM-5 catalyst was selected for further use in continuous hydrotreating process. The reactions were operated at temperature of 400°C, $H_2$ pressure of 40 bar, $H_2$/oil molar ratio of 100. The most suitable LHSV of 2 $h^{-1}$ condition was found to achieve high conversion (90.1%) and jet yield (40.6%) with a stable operation. The conversion gradually dropped over 80 h of the operating time (approx. 65.0% conversion) and then suddenly drops to 36.5% conversion at 103 h. It might be caused by coke deposition on surface catalyst of the catalyst. To examine the properties of the bio jet fraction, liquid products were distillated to obtain the jet range product. The distilled bio jet contained the net heat of combustion and aromatic volume of 42.29 MJ/kg and 24.49%, respectively which comply to ASTM D 1655 and ASTM D 7566.

## 6.2 Recommendations

1. The liquid products of continuous hydrotreating process with 12.5Ni2.5Cu on HZSM-5 had high aromatic content including alkylbenzene and toluene. After distillation, these components are mainly in lighter fraction. It is suggested to analyze a possibility of using this light fraction as a chemical solvent rather than gasoline fuel.
2. The properties of bio jet fuel such as density, viscosity, freezing point and the others should analyze to compare with ASTM D 1655 and ASTM D 7566. In this thesis does not report because the properties require high amount of bio jet fuel.

# REFERENCES


[1] de Sousa, F.P., Cardoso, C.C., and Pasa, V.M. Producing hydrocarbons for green diesel and jet fuel formulation from palm kernel fat over Pd/C. Fuel processing technology 143 (2016): 35-42.

[2] Diederichs, G.W., Mandegari, M.A., Farzad, S., and Görgens, J.F. Techno-economic comparison of biojet fuel production from lignocellulose, vegetable oil and sugar cane juice. Bioresource technology 216 (2016): 331-339.

[3] Wang, W.-C. Techno-economic analysis of a bio-refinery process for producing Hydro-processed Renewable Jet fuel from Jatropha. Renewable Energy 95 (2016): 63-73.

[4] Alternative Energy and Efficiency Information Center Department of Alternative Energy Development and Efficiency, M.o.E. Thailand Energy Statistics 2013. Thailand Energy Statistics (2013): 34-36.

[5] Michaelowa, A. and Jotzo, F. Transaction costs, institutional rigidities and the size of the clean development mechanism. Energy policy 33(4) (2005): 511-523.

[6] Kalayci, E., Gaygisiz, E., and Weber, G.-W. A multi-period stochastic portfolio optimization model applied for an airline company in the EU ETS. Optimization 63(12) (2014): 1817-1835.

[7] Corporan, E., et al. Chemical, thermal stability, seal swell, and emissions studies of alternative jet fuels. Energy & fuels 25(3) (2011): 955-966.

[8] Wang, S., Cai, Q., Wang, X., Zhang, L., Wang, Y., and Luo, Z. Biogasoline production from the co-cracking of the distilled fraction of bio-oil and ethanol. Energy & Fuels 28(1) (2013): 115-122.

[9] Chen, L., Li, H., Fu, J., Miao, C., Lv, P., and Yuan, Z. Catalytic hydroprocessing of fatty acid methyl esters to renewable alkane fuels over Ni/HZSM-5 catalyst. Catalysis Today 259 (2016): 266-276.

[10] Duan, P. and Savage, P.E. Hydrothermal liquefaction of a microalga with heterogeneous catalysts. Industrial & Engineering Chemistry Research 50(1) (2010): 52-61.

[11] De Rogatis, L., Montini, T., Cognigni, A., Olivi, L., and Fornasiero, P. Methane partial oxidation on NiCu-based catalysts. Catalysis Today 145(1) (2009): 176-185.

[12] Pimentel, D., et al. Food versus biofuels: environmental and economic costs. Human ecology 37(1) (2009): 1-12.

[13] Priyadarshani, I. and Rath, B. Commercial and industrial applications of micro algae–A review. J algal biomass utln 3(4) (2012): 89-100.

[14] Srifa, A., Faungnawakij, K., Itthibenchapong, V., Viriya-Empikul, N., Charinpanitkul, T., and Assabumrungrat, S. Production of bio-hydrogenated diesel by catalytic hydrotreating of palm oil over NiMoS 2/γ-Al 2 O 3 catalyst. Bioresource technology 158 (2014): 81-90.

[15] Peng, B., Zhao, C., Kasakov, S., Foraita, S., and Lercher, J.A. Manipulating catalytic pathways: deoxygenation of palmitic acid on multifunctional catalysts. Chemistry–A European Journal 19(15) (2013): 4732-4741.

[16] Greeley, J. and Mavrikakis, M. Surface and subsurface hydrogen: Adsorption properties on transition metals and near-surface alloys. Journal of Physical Chemistry B-Condensed Phase 109(8) (2005): 3460-3471.

[17] Kyriakou, G., et al. Isolated metal atom geometries as a strategy for selective heterogeneous hydrogenations. Science(Washington) 335(6073) (2012): 1209-1212.

[18] Greeley, J. and Mavrikakis, M. Surface and subsurface hydrogen: Adsorption properties on transition metals and near-surface alloys. The Journal of Physical Chemistry B 109(8) (2005): 3460-3471.

[19] Yao, Y. and Goodman, D.W. Direct evidence of hydrogen spillover from Ni to Cu on Ni–Cu bimetallic catalysts. Journal of Molecular Catalysis A: Chemical 383 (2014): 239-242.

[20] Duan, P. and Savage, P.E. Catalytic treatment of crude algal bio-oil in supercritical water: optimization studies. Energy & Environmental Science 4(4) (2011): 1447-1456.

[21] Benson, T.J., Hernandez, R., French, W.T., Alley, E.G., and Holmes, W.E. Elucidation of the catalytic cracking pathway for unsaturated mono-, di-, and triacylglycerides on solid acid catalysts. Journal of Molecular Catalysis A: Chemical 303(1) (2009): 117-123.

[22] Veriansyah, B., et al. Production of renewable diesel by hydroprocessing of soybean oil: effect of catalysts. Fuel 94 (2012): 578-585.

[23] Srifa, A., Faungnawakij, K., Itthibenchapong, V., and Assabumrungrat, S. Roles of monometallic catalysts in hydrodeoxygenation of palm oil to green diesel. Chemical Engineering Journal 278 (2015): 249-258.

[24] Zuo, H., Liu, Q., Wang, T., Ma, L., Zhang, Q., and Zhang, Q. Hydrodeoxygenation of methyl palmitate over supported Ni catalysts for diesel-like fuel production. Energy & Fuels 26(6) (2012): 3747-3755.

[25] Santillan-Jimenez, E., Morgan, T., Lacny, J., Mohapatra, S., and Crocker, M. Catalytic deoxygenation of triglycerides and fatty acids to hydrocarbons over carbon-supported nickel. Fuel 103 (2013): 1010-1017.

[26] Guo, Q., Wu, M., Wang, K., Zhang, L., and Xu, X. Catalytic hydrodeoxygenation of algae bio-oil over bimetallic Ni–Cu/ZrO2 catalysts. Industrial & Engineering Chemistry Research 54(3) (2015): 890-899.

[27] Dickinson, J.G. and Savage, P.E. Development of NiCu catalysts for aqueous-phase hydrodeoxygenation. ACS Catalysis 4(8) (2014): 2605-2615.

[28] Khromova, S.A., et al. Anisole hydrodeoxygenation over Ni–Cu bimetallic catalysts: The effect of Ni/Cu ratio on selectivity. Applied Catalysis A: General 470 (2014): 261-270.

[29] Sotelo-Boyas, R., Liu, Y., and Minowa, T. Renewable diesel production from the hydrotreating of rapeseed oil with Pt/Zeolite and NiMo/Al2O3 catalysts. Industrial & Engineering Chemistry Research 50(5) (2010): 2791-2799.

[30] Kiatkittipong, W., Phimsen, S., Kiatkittipong, K., Wongsakulphasatch, S., Laosiripojana, N., and Assabumrungrat, S. Diesel-like hydrocarbon production from hydroprocessing of relevant refining palm oil. Fuel processing technology 116 (2013): 16-26.

[31] Forzatti, P. and Lietti, L. Catalyst deactivation. Catalysis today 52(2) (1999): 165-181.

[32] Bartholomew, C.H. Mechanisms of catalyst deactivation. Applied Catalysis A: General 212(1) (2001): 17-60.

[33] Moulijn, J.A., Van Diepen, A., and Kapteijn, F. Catalyst deactivation: is it predictable?: What to do? Applied Catalysis A: General 212(1) (2001): 3-16.

[34] Chen, N., Gong, S., Shirai, H., Watanabe, T., and Qian, E.W. Effects of Si/Al ratio and Pt loading on Pt/SAPO-11 catalysts in hydroconversion of Jatropha oil. Applied Catalysis A: General 466 (2013): 105-115.

[35] Ala'a, H., et al. Efficient utilization of waste date pits for the synthesis of green diesel and jet fuel fractions. Energy Conversion and Management 127 (2016): 226-232.

[36] Zheng, X., Chang, J., and Fu, Y. One-pot catalytic hydrocracking of diesel distillate and residual oil fractions obtained from bio-oil to gasoline-range hydrocarbon fuel. Fuel 157 (2015): 107-114.

[37] Liu, M., et al. Seed-induced synthesis of hierarchical ZSM-5 nanosheets in the presence of hexadecyl trimethyl ammonium bromide. Rsc Advances 5(12) (2015): 9237-9240.

[38] Orojloo, M., Nourian, F., Arabahmadi, R., and Amani, S. Ni (II), Cu (II), AND Zn (II) Complexes derived from a new Schiff base 2-((Z)-(3-methylpyridin-2-yleimino) methyl) phenol and synthesis of nano sized metal oxide particles from these compounds. Química Nova 38(9) (2015): 1187-1191.

[39] Xue, N., et al. Understanding the enhancement of catalytic performance for olefin cracking: Hydrothermally stable acids in P/HZSM-5. Journal of catalysis 248(1) (2007): 20-28.

[40] Zhang, T., et al. Selective catalytic reduction of NO with NH 3 over HZSM-5-supported Fe–Cu nanocomposite catalysts: the Fe–Cu bimetallic effect. Applied Catalysis B: Environmental 148 (2014): 520-531.

[41] Yakovlev, V., et al. Development of new catalytic systems for upgraded bio-fuels production from bio-crude-oil and biodiesel. Catalysis Today 144(3) (2009): 362-366.

[42] Robertson, S., McNicol, B., De Baas, J., Kloet, S., and Jenkins, J. Determination of reducibility and identification of alloying in copper-nickel-on-silica catalysts by temperature-programmed reduction. Journal of catalysis 37(3) (1975): 424-431.

[43] Xu, Y., Liu, S., Guo, X., Wang, L., and Xie, M. Methane activation without using oxidants over Mo/HZSM-5 zeolite catalysts. Catalysis letters 30(1) (1994): 135-149.

[44] Chen, L., Lin, L., Xu, Z., Li, X., and Zhang, T. Dehydro-oligomerization of methane to ethylene and aromatics over molybdenum/HZSM-5 catalyst. Journal of catalysis 157(1) (1995): 190-200.

[45] Mahdavian, M., Fatemi, S., and Fazeli, A. Modeling and simulation of industrial continuous naphtha catalytic reformer accompanied with delumping the naphtha feed. International Journal of Chemical Reactor Engineering 8(1) (2010).

# Appendix

# Appendix A

## Calculation for catalyst preparation

A.1 Calculation of weight and volume of component for ZSM-5 synthesis (Si/Al mole ratio = 20)

Formula:

$SiO_2$ 1 mol : $Al(NO_3)_3$ 0.05 mol : TPABr 0.03 mol : $H_2O$ 60 mol

Example 1: Basis on $H_2O$ 6 mol

$SiO_2$ 0.1 mol : $Al(NO_3)_3$ 0.005 mol : TPABr 0.003 mol : $H_2O$ 6 mol

$SiO_2$ 0.1 mol : $0.1\ \text{mol} \times \frac{60\ \text{g}}{1\ \text{mol}} = 6\ \text{g}$

$Al(NO_3)_3$ 0.005 mol : $0.005\ \text{mol} \times \frac{375.13\ \text{g}}{1\ \text{mol}} = 1.876\ \text{g}$

TPABr 0.003 mol : $0.003\ \text{mol} \times \frac{266.26\ \text{g}}{1\ \text{mol}} = 0.79\ \text{g}$

$H_2O$ 6 mol : $6\ \text{mol} \times \frac{18\ \text{g}}{1\ \text{mol}} \times \frac{1\ \text{ml}}{1\ \text{g}} = 108\ \text{g}$

A.2 Ion Exchange: preparation of $NH_4NO_3$ 1 M in 100 ml $H_2O$

$NH_4NO_3$ 1000 ml : $NH_4NO_3$ 80 g

$NH_4NO_3$ 100 ml : $NH_4NO_3$ $80 \times \frac{100}{1000} = 8\ \text{g}$



A.3 Impregnation: preparation of 10Ni5Cu on 2 g. of HZSM-5 supported catalyst

$$2\ \text{g of (HZSM}-5) \times \frac{10\ \text{g of Ni}}{85\ \text{g of (HZSM}-5)} \times \frac{1\ \text{mol of Ni}}{58.69\ \text{g of Ni}} \times \frac{1\ \text{mol of Ni}(NO_3)_2 \cdot 6H_2O}{1\ \text{mol of Ni}} \times \frac{290.81\ \text{g of Ni}(NO_3)_2 \cdot 6H_2O}{1\ \text{mol of Ni}(NO_3)_2 \cdot 6H_2O} \times \frac{1}{0.97}$$
$$= 1.201\ \text{g of Ni}(NO_3)_2 \cdot 6H_2O$$

$$2\ \text{g of (HZSM}-5) \times \frac{5\ \text{g of Cu}}{85\ \text{g of (HZSM}-5)} \times \frac{1\ \text{mol of Cu}}{63.55\ \text{g of Cu}} \times \frac{1\ \text{mol of Cu}(NO_3)_2 \cdot 6H_2O}{1\ \text{mol of Cu}} \times \frac{241.6\ \text{g of Cu}(NO_3)_2 \cdot 6H_2O}{1\ \text{mol of Cu}(NO_3)_2 \cdot 6H_2O} \times \frac{1}{0.98}$$
$$= 0.456\ \text{g of Ni}(NO_3)_2 \cdot 6H_2O$$

## Appendix B

Calculation for acid density of catalyst

Calculation of the total acid sites by ammonia temperature program desorption ($NH_3$-TPD) is as following:

From the calibration curve of 15%$NH_3$ in Ar gas.

$$y = 36.093 \cdot x$$

y is concentration of acid

x is total peak area

Then: $\text{Acid density} = \frac{y}{weight\ of\ catalyst}$

Example 1:

total peak area = 1.221

weight of catalyst = 0.0548 g

$$\text{Acid density} = \frac{y}{\text{weight of catalyst}} = \frac{36.093 \times 1.221}{0.0548} = 0.802\ \text{mmol/g}$$

## Appendix C

Calculation for oxygen atoms removed of catalyst

Calculation of the oxygen atoms removed by hydrogen temperature program reduction ($H_2$-TPR) is as following:

From the AgO is standard

Basis: AgO could remove O of 100%

AgO 123.86 g : O 16 g

AgO 0.1 g : $\mathrm{O} = \frac{0.16 \times 0.1}{123.86} = 0.0129$ g

Weight of O = 0.0129 g

Molecular weight of O = 16 g/mol

Mole of O = 0.0129/16 = 0.0008074 mol

Area of Ag (from $H_2$-TPR) = 63.57 : O removed 0.0008074 mol

Example 1: 0.0850 g of 12.5Ni2.5Cu/HZSM-5 catalyst had total peak area of 100.79

Area of AgO 63.57 : O removed 0.0008074 mol

Area of catalyst 100.79 : $\mathrm{O\ removed} = \frac{0.0008074 \times 100.79}{63.57} = 0.0012801$ mol



$$\text{Amount of O removed} = \frac{\text{O removed}}{\text{weight of catalyst}} = \frac{0.0012801}{0.0850} = 0.01506 \text{ mol/g}$$

$$\text{Total of O removed} \left(\frac{\text{atoms}}{\text{g}}\right) = \text{Amount of O removed} \times \text{Avogadro's number}$$

$$\text{Avogadro's number} = 6.022 \times 10^{23} \text{ atoms/mol}$$

So: $\text{Total of O removed} \left(\frac{\text{atoms}}{\text{g}}\right) = 0.01506 \times 6.022 \times 10^{23} = 9.1 \times 10^{21} \frac{\text{atoms}}{\text{g}}$

# VITA

Mr. Phisit Wirikulcharoen was born on May 6, 1993 in Nakhonratchasima, Thailand. He graduated high school from Boonwatana School in 2011. He graduated with the Bechelor's degree in Chemical Engineering from Khon Kaen University in May 2015. Then, he entered to study the Master's Degree in Chemical Engineering at Department of Chemical Engineering, Faculty of Engineering, Chulalongkorn University, Bangkok Thailand since 2015 and completed the program in December 2017.